Aus der Klinik und Poliklinik für Kinder- u. Jugendpsychiatrie, Psychosomatik u. Psychotherapie

der Universität Würzburg

Direktor: Professor Dr. med. Marcel Romanos

Correlates of Substantia Nigra Echogenicity in Healthy Children

Inaugural - Dissertation

zur Erlangung der Doktorwürde der Medizinischen Fakultät der Julius-Maximilians-Universität Würzburg

vorgelegt von Sulamith Schaeff

aus

Bad Herrenalb

Würzburg, Juni 2019

Referent: Professor Dr. Marcel Romanos

Korreferentin: Privatdozentin Dr. Camelia-Maria Monoranu

Dekan: Professor Dr. Matthias Frosch

Tag der mündlichen Prüfung: 09.03.2021

Die Promovendin ist Ärztin

Contents

1 Introduction

1.1 Transcranial Sonography

Transcranial Sonography (TCS) has gained increasing importance since Aaslid, Markwalder and Nornes (1982) demonstrated the feasibility of Doppler ultrasound on adult cerebral arteries. Hitherto the adult skull was thought to be non-penetrable for ultrasound waves. The depiction of cerebral blood flow in adults with ultrasound was ground-breaking. Aaslid and colleagues (1982) placed the probe at the temporal bone region, where the skull is relatively thin and therefore the ultrasound signal is less diminished. They further minimized signal attenuation by reducing insonation frequencies to $2.0\,MHz$, common Doppler systems operate with $5 - 10\,MHz$. By modifying those parameters, Aaslid and colleagues (1982) successfully measured blood flow velocities in cerebral arteries. It was integrated quickly in clinical routines as it enables on-time and noninvasive monitoring of intracranial hemodynamic states as well as cerebrovascular disorders.

Diagnostic sonography is built on the piezoelectrical effect: electrical energy is converted into mechanical energy. When alternating current is applied, piezoelectrical crystals deform, vibrate and thereby send out ultrasound. Ultrasound is sound waves above $20,000\,Hz$, thus non audible for humans but e.g. for dolphins and bats. Different tissues reflect, disperse and absorb sound waves differently and as a result create distinct signals. These echoes hit again the piezoelectrical crystal with the reverse effect: mechanical energy is converted back into electrical energy. Amplitude, timing and pitch of the sound waves get recorded and images are calculated. Most commonly B-mode (brightness modulation) images are used where echo intensity is translated into scales of grey. Thus, image brightness of a certain pixel displays echo amplitude of a certain spatial point (Dössel, 2016). In this way different tissues and different brain areas e.g. brain stem and ventricular system can be depicted and measured (Becker et al., 1994a, 1995). Furthermore, noninvasive detection of pathological processes such as intracerebral malignoms and hemorrhagic events is possible (Becker et al., 1992, 1994b; Woydt et al., 1996).

In 1995, Becker and colleagues demonstrated structural differences of the substantia nigra (SN) with TCS in patients with Parkinson's disease (PD) and thereby gave directions to the use of TCS in neurodegenerative movement disorders. They observed an enhanced TCS signal of the SN in PD patients: SN was hyperechogenic compared to healthy subjects. SN, a mesenecephalic nucleus, is known amongst others to be involved in movement and the pathophysiology of PD (Bear, Connors & Paradiso, 2007).

Within the last years TCS has been widely used in neuropsychiatric movement disorders. Standardized protocols to assess midbrain structures in neurodegenerative diseases have been designed (Walter et al., 2007). Due to technical limitations, these days signal brightness can not be quantified directly. Therefore indirect measures have been developed to evaluate signal intensity. Two approaches are well-established: 1. planimetric measurement of an echogenic area or 2. semiquantitative rating of signal intensity by visual inspection (Walter et al., 2007). Consequently structures are defined as hypoechogenic if an echogenic area is smaller or lower in signal intensity compared to the general population. Hyperechogenicity describes the opposite: a greater area or higher signal intensity (Walter et al., 2007; Berg et al., 2008). Overall the brain parenchyma is mainly low in echogenicity. High echogenicity can be a result of i.e. calcium accumulations or high tissue density (Becker & Berg, 2001).

Sonography in general and TCS in particular is advantageous in many respects. It allows bedside examination of critically ill patients, it is noninvasive, fast, relatively low priced and widely available (Dössel, 2016). In neuropsychiatric movement disorders it is especially useful because motion (i.e. a moving patient) does not distort the entire measurement as it is the case in magnetic resonance imaging (MRI). Noninvasive MRI technique is based on spinning protons and magnetic properties of different tissues, its spatial resolution is high, but examinations take long and motion artefacts are common (Dössel, 2016). Sonography further permits an online mapping of dynamic changes, hence its temporal resolution is high. Besides, reliability of the measurements can be increased tremendously since numerous replications of measurements are viable (Skoloudík & Walter, 2010). Limitations are mainly due to particular characteristics of patients and the dependency on investigator's expertise. As

in conventional sonography, patients' physical features influence the quality of the TCS signal and images. In about $10 - 20$ % of Caucasians no adequate temporal bone window can be found, presumably due to variations in bone structure (Berg, Godau & Walter, 2008; Walter et al., 2007). In ethnic Asians the percentage is even higher varying between $21 - 59$ % (Kim et al., 2007; Okawa et al., 2007). In addition, investigators' knowledge and practice is crucial for reliable measurements (Skoloudík, 2007). And last, mainly structures near the midline are explorable and superficial brain structures near the skull cannot be displayed clearly (Skoloudík & Walter, 2010).

1.2 Transcranial Sonography in Movement Disorders

TCS is useful in neuroimaging of subcortical structures and detecting structural alterations. It has been used in a variety of movement disorders and reference values have been developed. Commonly in adults SN echogenic sizes of less than $.20\ cm^2$ are considered to be normal, SN sizes of $.20\ cm^2$ and above represent the upper $75\ percentile$ of the healthy population and are assumed to be hyperechogenic. But exact measures also depend on the ultrasound system used (Berg et al., 2008; Walter et al., 2007).

TCS in Parkinson's Disease PD was the first neuropsychiatric movement disorder where TCS was found to be a potentially useful diagnostic tool (Becker et al., 1995). Parkinsonism is a general term for hypokinetic syndromes with extrapyramidal key symptoms of hypokinesia, resting tremor, postural instability and rigidity. Parkinson's Disease refers specifically to the idiopathic form of parkinsonism. Besides, there are many secondary and acquired parkinsonian syndromes as well as so called atypical parkinsonian syndromes. PD is a common neurodegenerative disorders of the elderly, affecting $1 - 5$% of senior adults. PD is characterized by a loss of dopaminergic neurons in the pars compacta of the SN, a subsection of the SN and main source of dopamine (Lücking et al., 2013). Dopamine is a catecholaminergic neurotransmitter and involved in circuits of motor control (Bear, Connors & Paradiso, 2007).

In about 90% of PD patients SN is found to be hyperechogenic in TCS examination. Early findings of SN hyperechogenicity have been replicated numerously by independent groups and in different ethnicities (Becker et al., 1995; Berg et al., 2008; Gaenslen et al., 2008; Kim et al., 2007; Okawa et al., 2008). Apparently this hyperechogenicity is a trait marker, it does not reflect disease severity (Spiegel et al., 2006) nor does it progress over time (Berg et al., 2005). Therefore TCS has been proposed as a diagnostic tool in early diagnosis of PD when symptoms are not yet fully developed and accurate diagnosis can be complex (Gaenslen & Berg, 2010). Other studies though did not find satisfactory sensitivity and specificity to enable classification (Bouwmans, 2013).

Another clinical application might be the differentiation between idiopathic PD and atypical parkinsonian syndromes. Atypical parkinsonian syndromes usually involve a multisystem degeneration. They have clinical symptoms in addition to the typical parkinsonian malfunctions and are therefore also called Parkinson-plus syndromes. Often patients are younger at disease onset, symptoms are more severe and the course of the disease is more rapid. Moreover, atypical parkinsonian patients respond poorly to levodopa (L-Dopa), which is a precursor of dopamine and the standard medication in PD. Examples for atypical syndromes include multiple system atrophy which is also associated with autonomic dysfunctions and progressive supranuclear palsy which is marked i.e. by vertical gaze palsy (Lücking et al., 2013). Especially in early disease stages classification can be a challenge and differentiation from idiopathic PD is delicate (Caslake et al., 2008). Postmortem studies reveal false positive rates in diagnosing idiopathic PD around 25% at the expense of under-diagnosing atypical parkinsonian syndromes (Joutsa et al., 2014). Evidently, patients would benefit from a reliable imaging marker. Clear categorization is not a mere scientific question but is of great importance for adequate treatment. Hyperechogenic SN might be such a marker, it is distinctive for idiopathic PD. Good sensitivity, specificity and predictive values have been obtained in order to distinguish idiopathic PD and atypical syndromes by means of TCS (Berg et al., 2008; Gaenslen et al., 2008).

TCS in Huntington's Disease Huntington's disease (HD) is a trinucleotide repeat disorder with expanded cytosine-adenine-guanine (CAG) repeats. HD is characterized by initial hyperkinetic symptoms and in later stages hypokinesia and dementia. It is known to cause GABAergic cell loss, the main inhibitory neurotransmitter. Besides, it is accompanied by atrophies in different brain regions i.e. striatum, thalamus, substantia nigra and cerebral cortex. HD is a genetic disease and with increasing numbers of CAG repeats, anticipation is a well known effect. Anticipation refers to an aggravation of symptom severity and earlier disease onset (Lücking et al., 2013). Interestingly, in an early study Postert and colleagues (1999) found a positive correlation between SN hyperechogenicity and symptom severity as well as number of CAG repeats. Nevertheless, this was only true for about 40 % of their HD patients. Recently, SN hyperechogenicity has been demonstrated in more than 90 % of HD patients when priorly screened for hypokinetic symptoms. This indicates that SN alterations might be specific in a subgroup of HD patients with hypokinesia (Lambeck et al., 2015).

TCS in Restless Legs Syndrome Restless legs syndrome (RLS), a hyperkinetic syndrome, is marked by an urge to move the legs and dysesthetic sensations. Usually symptoms diminish when moving around and worsen when the patient rests. An underlying dysfunction of the dopaminergic system is proposed and supported by the fact that RLS is effectively treated with levodopa or dopamine agonists (Lücking et al., 2013). As in other movement disorders echogenic signals of the SN are altered. SN demarcates hypoechogenic in TCS in most idiopathic RLS patients as compared to healthy subjects. The signal is thus diminished (Godau & Sojer, 2010; Schmidauer et al., 2005). Also RLS symptom severity correlates negatively with hypoechogenicity of the SN in patients with neurodegenerative movement disorders and comorbid RLS (Pedroso et al., 2012).

TCS in Attention-Deficit Hyperactivity Disorder Attention-deficit hyperactivity disorder (ADHD) is not a generic movement disorder, nevertheless it is characterized by excess motor activity. ADHD is a common hyperkinetic disorder

with prevalences around $8 - 10\,\%$ and by definition begins in childhood. Besides striking motor activity, patients exhibit psychomotor restlessness, impulsivity and have difficulties in sustaining attention. ADHD has a strong hereditary component, often persists into adulthood and its prevalence is more than doubled in boys (Bokor & Anderson, 2014). Subcortical alterations i.a. in the basal ganglia have been found in ADHD boys but not in girls (Seymour et al., 2017; Qiu et al., 2009) and also in both sexes (Shaw et al., 2014). Nigral dopaminergic malfunction has been proposed as part of the underlying pathophysiology, which is not yet thoroughly understood (Badgaiyan et al., 2010; Biederman & Faraone, 2005; Bokor & Anderson, 2014). Based on altered nigral echogenicity in PD and common pathophysiological pathways, TCS has been performed on ADHD patients. Nigral TCS signal is markedly hyperechogenic in ADHD children and adolescents as compared to healthy controls (Krauel et al., 2010; Romanos et al., 2010). Analogous to PD patients $mean$ SN sizes of $.20\ cm^2$ have been reported in ADHD children (Romanos et al., 2010). SN echogenic size also correlates with symptom severity of inattention, hyperactivity and impulsivity (Krauel et al., 2010). The occurrence of SN hyperechogenicity in other typic movement disorders hints at the motor component of ADHD and TCS suggests morphological changes of the SN. Hyperechogenicity of the SN might serve as a structural marker for ADHD.

1.3 Iron Metabolism in Movement Disorders

It is not only, that movement disorders share striking echographic findings of the substantia nigra as described before. The following chapter will outline that the substantia nigra in turn is closely intertwined with aberrant cerebral iron and movement disorders.

Substantia nigra The SN is part of a complex regulation network involved in motion, addiction, learning, the reward system and others. It is located in the tegmentum of the mesencephalon. Functionally and structurally the SN is divided into two nuclei: pars compacta and pars reticulata. The pars compacta contains

neuromelanin-pigmented dopaminergic neurons, it is dark in color and responsible for its illustrative name 'substantia nigra'. The nigrostriatal pathway is formed by axons that project anteriorly to the striatum. The pars reticulata comprises inhibitory GABA-ergic (γ-aminobutyric acid) neurons, receives direct and indirect input from the striatum and projects in turn to the thalamus (Gazzaniga, Ivry & Mangun, 2009). Dopamine is known to be involved in different projections and neural pathways regarding motor control, reward, sleep, attention and memory processes. Motion processes in particular are mediated by dopaminergic projections from the substantia nigra pars compacta. Dopamine is synthesized through enzymatic reactions from tyrosine via L-Dopa to dopamine within the catecholaminergic pathway (Bear, Connors & Paradiso, 2007). Interestingly, movement disorders with dopaminergic dysfunction such as PD or ADHD are more frequent among males. Sex hormones and sex genes are proposed to mediate dopamine synthesis (Loke, Harley & Lee, 2015). Neuromelanin in the central nervous system partly resembles cutaneous melanin. It is a brownish pigment produced and contained in catecholaminergic neurons in some areas of the brain, but mainly in the SN pars compacta. Neuromelanin is also synthesized within the catecholaminergic pathway. Its concentration is thus dependent on catecholamine synthesis. Neuromelanin binds metals such as iron, copper, zinc and thereby presumably functions as protective antioxidant. In PD the buffering system in not intact, dopaminergic neurons containing neuromelanin are lost. (Fedorow et al., 2005, Zecca et al., 2002).

Cerebral Iron Non-heme iron is abundant within the central nervous system, in some brain areas quantities are even comparable to the liver. Highest concentrations are measured i.a. within the SN. Cerebral iron is contained in transport and structural proteins, enzymes and in iron storage proteins such as ferritin. It is also pooled in neuromelanin (Beard & Connor, 2003; Singh et al., 2014). Whereas ferritin is mostly found in glia cells, in dopaminergic neurons of the SN neuromelanin appears to be a storage system of iron (Fedorow et al., 2005, Zecca et al., 2002). The blood-brain barrier keeps cerebral iron partly independent of the rest of the body and maintains homeostasis. Thus, normal

serum iron concentrations do not mean normal cerebral iron or vice versa, if anything their concentrations differ. Iron is indispensable for brain function, it is amongst others involved in myelination, enzyme synthesis as well as synthesis and catabolism of neurotransmitters such as dopamine. Iron is an essential coenzyme of tyrosine hydroxylase, the rate-limiting enzyme in catecholamine or dopamine synthesis. Iron and dopaminergic neurons are co-located within the substantia nigra and functionally associated. Shortage of cerebral iron is associated with a decrease in dopamine transporters and receptors. On the other hand, free iron is cytotoxic, it reacts with molecular oxygen. Iron homeostasis is complex and depends on requirements, resorption, distribution and storage (Beard & Connor, 2003; Singh et al., 2014).

Iron and Movement Disorders In PD patients the SN shows signs of iron dysfunction. Not only loss of neuromelanin, but also abnormally high iron concentrations in the SN pars compacta have been found repeatedly. It has been proposed that iron excess leads to oxidative stress causing dopaminergic cells to decline, but it remains a matter of debate, whether it is cause or consequence (Dexter et al., 1989; Gerlach et al., 1994; Götz et al., 2004).

In ADHD scientific evidence is controversial. Depending on the study design lower serum ferritin levels have repeatedly been found to be related to hyperactivity and symptom severity in ADHD (Juneja et al., 2010; Oner, Alkar & Oner, 2008; Oner et al., 2012). Though others did not find an association (Adisetiyo et al., 2014; Donfrancesco et al., 2013). Recent MRI studies show significantly lower iron indices in striatum and thalamus in ADHD patients as compared to healthy controls (Adisetiyo et al., 2014; Cortese et al., 2012). Moreover, these differences are only evident in medication-naive ADHD patients, suggesting that altered cerebral iron indices map dopaminergic disruption, which is reversible with medication. (Adisetiyo et al., 2014; Adisetiyo & Helpern, 2015). In fact, ADHD psychostimulant medication is known to increase dopamine levels (Del Campo et al., 2011).

Research on RLS also pinpoints the role of iron metabolism in its pathogenesis. Iron deficiency increases the risk of developing RLS. Furthermore, symptoms

can be alleviated by intravenous iron treatment, even if patients are not deficient in iron (Allen & Earley, 2007). MRI measurements of nigral iron concentrations are negatively correlated with symptom severity (Allen et al., 2001). In idiopathic RLS patients ferritin concentrations of the cerebrospinal fluid are significantly lower, whereas transferrin levels of cerebrospinal fluid are higher when compared to healthy subjects. This suggests a central iron deficiency and altered blood-brain barrier transport mechanisms. (Earley et al., 2000, Mizuno et al., 2005). The findings correspond with necropsies on RLS brains, that show decreased immunostaining of ferritin and increased staining of transferrin in the SN (Connor et al., 2003). Iron might also be a link to the proposed dopaminergic dysfunction in RSL and PD, since it influences dopamine metabolism and dopaminergic signal transmission (Allen & Earley, 2007; Connor et al., 2003).

1.4 Substrates of Substantia Nigra Hyperechogenicity

As stated previously, the SN is found to be hyperechogenic in some medical conditions such as PD or ADHD. But nigral hyperechogenicity is also detected in up to 10 % of healthy adults (Berg et al., 1999a; Schweitzer et al., 2007). On the other hand, in RLS the SN demarcates hypoechogenic. Underlying biological mechanisms of SN echogenicity remain unclear. However, there is preliminary evidence for the role of iron in echogenic alterations.

Findings from Movement Disorders Insights come from research on neurodegeneration with brain iron accumulation (formerly Hallervorden-Spatz syndrome). This is a group of orphan genetic diseases. Core symptoms include gait abnormalities, rigor, dysarthria and dystonia (Dashti & Chitsaz, 2014). Pathological iron deposits i.e. in the SN are known to be involved in its pathophysiology (Koeppen & Dickson, 2001). Commonly it is diagnosed clinically and in addition with genetic testing and MRI. But MRI measurements in patients with movement disorders, especially in children, are troublesome. Patients have to be sedated in order to avoid motion artefacts. Moreover, pathognomonic abnormalities are sometimes but not always depicted in MRI

images (Liman et al., 2012). Therefore it is auspicious that nigral structural abnormalities are also visible in TCS. Albeit small sample size, the results are promising. In planimetric measurements SN hyperechogenicity was found in all 7 patients and size differences ($mean$ size right SN .39 cm^2 and left SN .35 cm^2) compared to healthy controls ($mean$ size right SN .12 cm^2 and left SN .10 cm^2) were highly significant. The correspondence between the two neuroimaging methods as well as neuropathological results suggest a potential connection between iron deposits and nigral echogenicity (Liman et al., 2012).

Findings from Neurologically Healthy Subjects In animal studies direct injection of iron into the SN of rats leads to a dose-dependent enhancement of SN echogenicity. This seems to be a special attribute of free iron. Direct injection of ferritin, that is protein-bound iron, has no effect on SN echogenicity. On the other hand injection of substances, that release iron from its storage molecule ferritin, leads to increases in echogenicity (Berg et al., 1999b).

Furthermore, a postmortem study of Zecca and colleagues (2005) found significant correlations between nigral echogenicity and iron-related parameters in human brains. They examined 40 brains of subjects without movement disorders and 3 PD brains. After removal from the skull TCS was performed on the brains and SN echogenicity was determined. Subsequently, SN was dissected and contents of ferritin, iron and neuromelanin were quantified for each subject. Results showed significant positive correlations between SN echogenicity and concentrations of iron as well as ferritin. On the other hand, neuromelanin was negatively correlated with SN echogenicity. Considering that neuromelanin incorporates iron and that their opposing effects on echogenicity might overlap, neuromelanin was only statistically significant, when iron concentrations had been taken into account as well. Previous findings on PD brains were replicated: hyperechogenic SN, elevated iron, reduced neuromelanin in the SN. In accordance with the animal model (Berg et al., 1999b) and rather weak correlations of ferritin, it has been discussed that lower levels of neuromelanin together with elevated iron content (but not ferritin) are related to SN echogenicity. And that those alterations in turn might express a toxic milieu and increased susceptibility for

nigrostriatal damage (Zecca et al., 2005).

If SN signal alterations in neurologically healthy and affected subjects underly the same cerebral changes and if these changes are due to iron abnormalities, questions about its implications raise. Hyperechogenicity in non-symptomatic and symptomatic subjects might be regarded as a marker for nigrostriatal disruption. Insights come from positron emission tomography (PET) studies on healthy subjects. Despite normal motor abilities, PET reveals reduced fluorine-18-dopa (^{18}F-dopa) uptake in the striatum in healthy subjects with hyperechogenic SN. PET is used for nuclear functional imaging and maps metabolic processes. Thus morphological changes might map functional changes: SN hyperechogenicity seems associated with decreased dopaminergic uptake in the striatum (Behnke et al., 2009; Berg et al., 1999a, 2002). Reduced ^{18}F-dopa uptake has also been reported in PD patients with nigral hyperechogenicity. Moreover, corresponding structural changes of the SN have been observed with MRI in patients and healthy subjects with hyperechogenic SN (Behnke et al., 2009). It has been suggested that SN hyperechogenicity can serve as a marker for nigrostriatal impairment and vulnerability in preclinical settings and PD patients (Behnke et al., 2009; Berg et al., 1999a, 2002).

The evidence for iron as the biological correlate of SN echogenicity is compelling. As outlined above, evidence suggests it is a multi-layered process consisting of aberrant iron deposits and altered iron handling mechanisms that depict enhanced vulnerability of nigrostriatal pathways. Still there are controversies and unanswered questions. About 90% of PD patients show SN hyperechogenicity (Berg et al., 2008; Walter et al., 2007). Reciprocally, the question arises whether the remaining 10% have no disturbances in SN iron metabolism. PD is known for SN iron overload (Dexter et al., 1989; Gerlach et al., 1994; Götz et al., 2004) and hyperechogenicity (e.g. Becker et al., 1995; Berg et al., 2008), whereas RLS is associated with SN iron deficiency (Allen et al., 2001; Connor et al., 2003) and SN hypoechogenicity (Godau & Sojer, 2010; Schmidauer et al., 2005). But PD patients with and without comorbid RLS do not differ in their degree of SN echogenicity (Ryu, Lee & Baik, 2011). Clearly, more research is warranted in order to illuminate the complex mechanisms underlying TCS signals in nigral echogenicity.

1.5 Transcranial Sonography of the Substantia Nigra in Children

Although TCS is an integral part of premature infant diagnostics in evaluating vessels, intracerebral bleedings and the ventricular system (Speer, 2013), there is only very limited research on midbrain structures in children. Hitherto to my best knowledge, 4 studies have been published assessing nigral echogenicity in children. Two studies focused on age-related changes in SN echogenicity (Hagenah et al., 2010; Iova et al., 2004) and, as mentioned before, 2 other independent studies addressed nigral echogenic signals in ADHD (Krauel et al., 2010; Romanos et al., 2010).

Evidence for the effects of age on SN echogenicity is conflicting. A gradual decrease of SN echogenicity with age has been found, with newborns exhibiting significantly greater SN echogenic areas than older children (Iova et al., 2004). Here, 77% of the infants (aged 12 months or younger) showed SN echogenic sizes over .19 cm^2, whereas by the age of 10 years this was only the case in about 17% of the children. Both proportion of hyperechogenicity (Berg et al., 1999a; Schweitzer et al., 2007) and cut-off scores for hyperechogenicity approach adult numbers (Walter et al., 2007). On the other hand, Hagenah and colleagues (2010) observed a significant increase in SN echogenic size with age. Their investigation included neurologically healthy infants/children from $0 - 17$ years as well as adults $23 - 72$ years. Here, lowest $mean$ SN measures for infants and children (.06 cm^2) and highest values for older subjects (.13 cm^2) were detected. Though subanalysis of the infants/children group did not reveal a significant correlation of age and SN echogenic size within this subcluster. In both TCS studies on ADHD age did not exert an effect on SN echogenic sizes (Krauel et al., 2010; Romanos et al., 2010). However, age range in the research designs was restricted to children from $6 - 17$ years and $7 - 16$ years respectively. As stated above, SN echogenic sizes are markedly pronounced in ADHD children as compared to healthy peers (Krauel et al., 2010; Romanos et al., 2010). Noticeable, SN echogenic sizes of the controls differed considerably between the two ADHD studies, although the

same ultrasound system was used. Whereas one study reported $mean$ sizes of .14 cm^2 (right) and .16 cm^2 (left) (Romanos et al., 2010), the other mentioned $median$ sizes of .40 cm^2 (Krauel et al., 2010). Likewise in the patient groups: $mean = .20\ cm^2$ and $median = 1.0\ cm^2$ respectively.

Since iron metabolism has been related to echogenic signals in adults, it stands to reason that it is also involved in potential temporal signal changes and nigral echogenicity in children. Consequently, altered brain iron metabolism and nigrostriatal vulnerability have been discussed (Iova et al., 2004; Krauel et al., 2010; Romanos et al., 2010). Aside from that, iron in the SN is known to accumulate over time, newborns have lowermost iron contents (Snyder & Connor, 2009; Zecca et al., 2004). Neuromelanin emerges first during the second/third year of life in the SN and its concentration increases with normal ageing (Zecca et al., 2001; Zucca et al., 2006). Though ambiguous age-related changes in echogenicity have been observed in children, in elderly subjects (Berg et a., 2001b) and PD patients (Berg et al., 2005) no effect of age has been found on SN echogenicity. It has been proposed that nigral hyperechogenicity develops early in life and afterwards changes are only subtle (Berg et al., 2001b). Consequently, depending on the range of age in the study design, correlations are visible or not (Hagenah et al., 2010). In ADHD evidence for iron as structural correlate is antithetic, albeit recent MRI data show in fact aberrant brain iron indices in ADHD. However, MRI shows iron deprivation in the striatum and thalamus (Adisetiyo et al., 2014; Donfrancesco et al., 2013), while from a TCS point of view one would rather expect iron overload from adult studies. Underlying biophysics of echogenicity might be a complex interaction of neuromelanin and iron contents, it might be different for ADHD and PD and possibly also related to the different age groups. Alternative hypotheses such as maturational delay and altered connectivity have been discussed elsewhere (Drepper et al., 2017).

In children scientific data on midbrain TCS are rare and moreover ambiguous. To enable a better interpretation of future patient data and a more profound understanding of the biological basis of the nigral TCS signal, reference values and conclusive data of the temporal dynamics in a clinically healthy population of children are desirable.

1.6 Multimodal Assessment of Nigral Echogenicity in Healthy Children

To recap shortly, hyperechogenic SN is found in about 10% of healthy adults (Berg et al., 1999a; Schweitzer et al., 2007) as well as different movement disorders (see chapter 1.2 for references). SN hyperechogenicity has been suggested to map nigrostriatal dysbalance in preclinical and clinical settings i.e. in the healthy population and in patients (Behnke et al., 2009; Berg et al., 1999a, 2002). In adults signal alterations might reflect high concentrations of nigral iron and low levels of neuromelanin. Nigral hyperechogenicity, thus, could be a marker of neuromelanin depletion and iron deposition expressing susceptibility for nigrostriatal impairment (Zecca et al., 2005). In addition, iron seems a plausible candidate, it is involved in the pathophysiology of many movement disorders (Snyder & Connor, 2009) and also in dopamine synthesis and transmission (Beard & Connor, 2003; Singh et al., 2014). In children though, research is sparse and within itself controversial. In healthy children increases of SN echogenicity with age have been reported (Hagenah et al., 2010) as well as decreases (Iova et al., 2004). ADHD is associated with SN hyperechogenicity (Romanos et al., 2010; Krauel et al., 2010). Structural correlates of SN echogenicity, at least in ADHD children, might be different from those in adults. MRI studies show diminished iron content in striatum and thalamus (Adisetiyo et al., 2014; Donfrancesco et al., 2013).

To my knowledge no studies have been made to further explore nigral echogenicity in healthy children. Up to now distribution of SN echogenicity and prevalences of SN hyperechogenicity in a healthy children population have not been investigated conclusively. It is of special interest how SN echogenicity relates to subclinical hyperactive behavior in healthy children. There is evidence in adults, that those who differ in structure also differ in motor function. In non-PD adults SN hyperechogenicity is associated with motor slowing (Berg et al., 2001b) and more severe extrapyramidal side effects under neuroleptic treatment (Berg et al., 2001a). It is then expected that in healthy children SN hyperechogenicity is also associated with more "hyperactive" behavior. Furthermore, the role of iron and neuromelanin in SN echogenicity of healthy children has not been resolved.

Recent technological advances have made non-invasive, indirect measurements of neuromelanin possible. Since neuromelanin binds e.g. iron it has paramagnetic effects rendering MRI feasible. In healthy adults nigral neuromelanin content and consequently in PD patients depletion of nigral neuromelanin can be visualized with neuromelanin-sensitive MRI (Sasaki et al., 2006; Ogisu et al., 2013; Ohtsuka et al., 2013). The relation between age and neuromelanin content of the SN has lately been investigated with neuromelanin-sensitive MRI: nigral neuromelanin measures rise gradually until the mid-fifties and decline afterwards (Xing, 2018). This is also in line with some neuropathological studies (Mann & Yates, 1978), whereas others report a lifelong increase (Zecca et al., 2001). Accordingly, it is presumed that SN hyperechogenicity in healthy children is associated with lower neuromelanin indices of the SN in neuromelanin-sensitive MRI and that the nigral neuromelanin measures show an age-dependent increase.

In an attempt to evaluate potential correlates of SN echogenicity in healthy children, the following multimodal study was conducted. Since direct measurements of cerebral iron are not ethical, a combination of indirect measures was employed. Neuroimaging techniques i.e. neuromelanin-sensitive MRI and TCS were combined with behavioral data from questionnaires and serum measures of iron-related parameters in healthy children. The aim of this study was to investigate ① the distribution of SN echogenicity and a critical value for SN hyperechogenicity in healthy children, ② whether nigral neuroimaging signals change over time and show an association with the age of the children, ③ whether SN echogenicity is correlated with hyperactive behavior in healthy children, and in addition, ④ whether SN echogenicity can be predicted by neuromelanin-sensitive MRI measures of the SN but not by peripheral iron status.

2 Methods

2.1 Participants

Between October 2013 and February 2015 a total of 34 healthy participants (4 females, 30 males) participated in this study of the Department of Child and Adolescent Psychiatry of Wuerzburg University Hospital (KJPPP). All participants were Caucasian. Requirements to participate included: age of $8-12$ years, IQ above 85 points, no psychiatric illness and no severe somatic illness (e.g. epilepsy, hyperthyroidism, diabetes, foetal alcohol syndrome, brain trauma). Furthermore, metal implants, pacemaker or dental braces and claustrophobia were criterions for exclusion since MRI measurements were also part of the study. Participants and their legal guardians received written information about course and purpose of the study before hand. Written informed consent was obtained from all participants as well as their legal guardians. Participants were recruited from a pool of healthy controls that participated recently in other studies of the KJPPP. They received a financial gratification for their participation. The ethics committee of Wuerzburg University gave their approval to this study (file reference 313/13) and it was conducted according to the standards of the Helsinki declaration.

2.2 Psychological Assessment

To assess psychological phenotype, standardized instruments were used. Since the children participated in other studies of the KJPPP within the last 6 months, no major changes in phenotype could be expected. Therefore the following data could be retrieved from a database of the KJPPP and did not have to be acquired once again.

CFT-20-R: For overall intelligence, intelligence quotient was measured using Culture Fair Intelligence Test, CFT-20-R (WeiSS, 2006). CFT-20-R comprises 101 items composed of 4 categories: series, classification, matrices and topology. Adequate scientific value is proven by high test-retest reliability ($= .80 - .82$), internal consistency ($= .95$) and good concurrent validity with other IQ tests ($mean = .64$). It assesses nonverbal intelligence in terms of fluid intelligence as defined by Cattell. Cattell distinguishes fluid and crystallized intelligence. Fluid intelligence corresponds to problem solving behavior independent of prior knowledge - thus novel situations. On the other hand crystallized intelligence relies on acquired skills and previous knowledge (e.g. Cattell, 1968).

SDQ-Deu: To evaluate psychological attributes and behavior,
Strength and Difficulties Questionnaire (SDQ) for parents (Goodman, 1997), was evaluated. The German version with German normative data (SDQ-Deu) was implemented (Woerner et al., 2002). Reliability is high ($Cronbach's\ \alpha = .82$) and concurrent validity with other questionnaires (amongst others Child Behavior Checklist) is good ($r = .78 - .83$) (Klasen et al., 2003). SDQ-Deu is a behavioral screening checklist that looks for psychological attributes. It consists of a total of 25 items regarding child behavior as rated by their parents. It examines emotional problems, conduct problems, problems with peers, hyperactivity and prosocial behavior. Each of these five subscales evenly contains 5 items and each item is rated on a 3-point scale (not true, somewhat true, certainly true). Final results are given as $percentiles$ in relation to a representative reference group. Higher scores indicate more problems: $< 80 = normal$, $\sim 80 - 90 = borderline$, $\gtrsim 90 = conspicuous$. Only children showing no evidence of psychiatric disorders ($total \leq 90th\ percentile$) were finally included.

2.3 Transcranial Sonography

TCS was performed using an Esaote Mylab25 Gold ultrasound system (Esaote S.p.A., Genoa, Italy) with a $2.5\,MHz$ phased array transducer. Penetration depth was set to $15.0\,cm$ and a dynamic range of $45\,dB$. Both parameter settings have been proven to be most appropriate for TCS in these kinds of settings (Berg et al., 2001b; Walter, 2012). Image brightness had to be adapted for each participant individually. Two-dimensional B-mode images of the brain were generated.

Axial images of standardized midbrain and diencephalic scanning planes were obtained, frozen and stored digitally for further analysis. TCS is performed through the intact scull at the temporal acoustic bone window on each side of the head respectively. The same examiner (S.S.) obtained and analyzed all TCS images. Quality and clearness of TCS images of diencephalic and mesencephalic structures strongly depend on the quality of the temporal acoustic bone window (Walter et al., 2007) making it crucial to find an optimal probe position. To this end, the exact position of the ultrasound probe had to be aligned for each participant individually. For offline analysis multiple pictures of each scanning plane were stored digitally. Among those a total of 4 pictures for each subject (midbrain left and right, diencephalon left and right) were chosen for subsequent investigation. Three participants had insufficient left temporal acoustic bone windows. Therefore analyses of these participants were limited to their right hemisphere.

Further analysis was done using ImageJ, an open source processing and analysis software based on Java by Wayne Rasband of the National Institute of Mental Health at National Institute of Health (Rasband, 1997). For precise evaluation pictures were zoomed-in $2 - fold$. Scanning planes can be identified and delineated by certain anatomical landmarks (Huber, 2010; Walter et al., 2007). Evaluation of brain structures was conducted according to standard procedures (Berg et al., 2008; Walter et al., 2007).

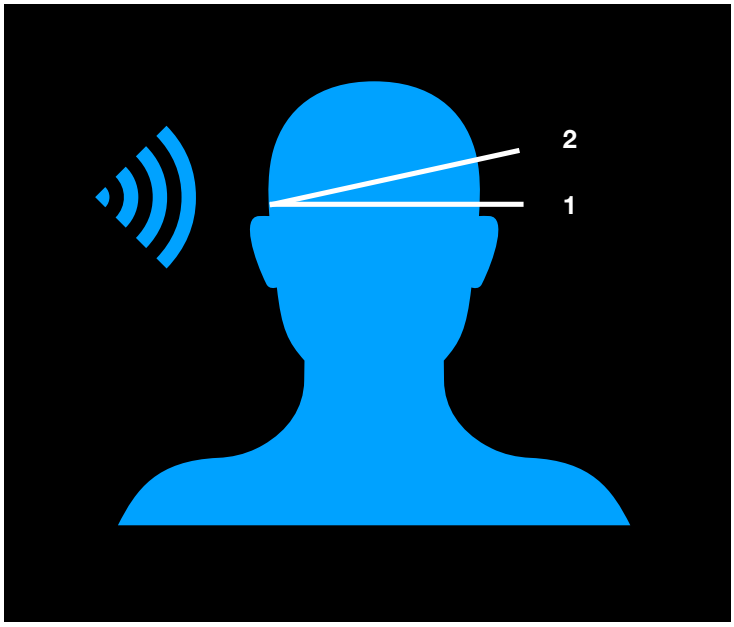

Figure 2.1: Scanning planes: 1 midbrain plane, 2 diencephalon plane.

Midbrain: By pressing the ultrasound probe firmly parallel to an imagined orbitomeatal line in the preauricular region, the midbrain level can be identified (see figure 2.1). It is marked by the butterfly-shaped mesencephalic brainstem, which is low in echogenicity, contrasting the surrounding highly echogenic basal cisterns (Huber, 2010; Walter et al., 2007). Within the midbrain the ipsilateral SN can be differentiated by its echogenicity at its anatomical site (Walter, 2012). Here, ipsilateral refers to the side of the probe: left SN is evaluated if the probe is positioned on the left side of the head and vice versa. Figure 2.2 shows an example of the pictures derived. Using ImageJ (Rasband, 1997), planimetric measurements of the brainstem and ipsilateral SN echogenic area were performed in double magnification. Measurement was effected through manually encircling the outer circumferences and subsequently calculating the size of each echogenic area automatically. Hitherto, this procedure has proven to be the best validated method (Walter, 2012).

Diencephalon: After identification of the midbrain level, the diencephalic scanning plane is found by tilting the probe about 10 degrees upwards (see figure 2.1). Here, the oval and low echogenic structures of the thalamus as well as the third ventricle are visible (Huber, 2010; Walter et al., 2007). Figure 2.3 displays an exemplary TCS image of the diencephalic plane. Further examination was conducted again in double magnification using ImageJ (Rasband, 1997). To scan for irregularities, contralateral thalamus was rated semiquantitatively. This was done by visually judging its echogenicity relative to the surrounding parenychma: normal echogenicity (i.e. hypo-or isoechogenic) versus hyperechogenicity (Postert at al., 1999; Walter et al., 2007). Furthermore, to rule out gross signal abnormalities the diameter of the third ventricle was determined by measuring maximum transverse diameter (from ipsilateral to contralateral) in-between the hyperechogenic ependymal confining contours. Width should not exceed 7 mm in adults $20 - 60$ years (Walter et al., 2007).

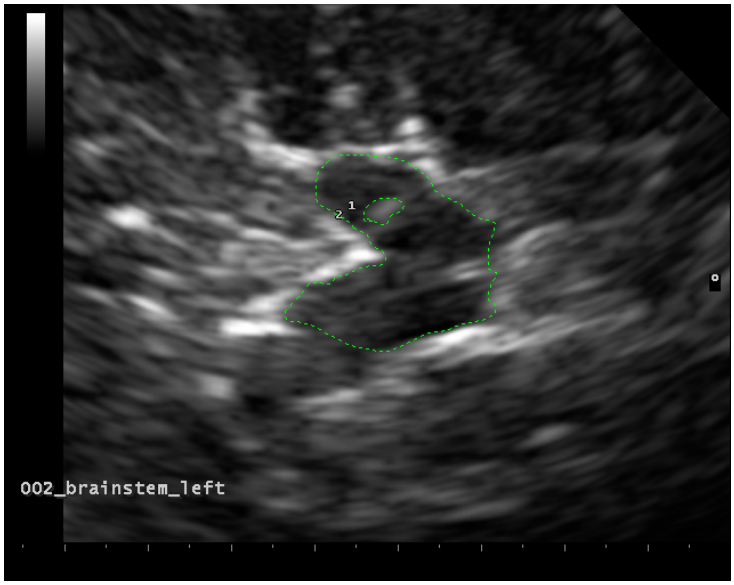

Figure 2.2: Midbrain level: brainstem (2) and substantia nigra (1) are manually encircled (green dotted line).

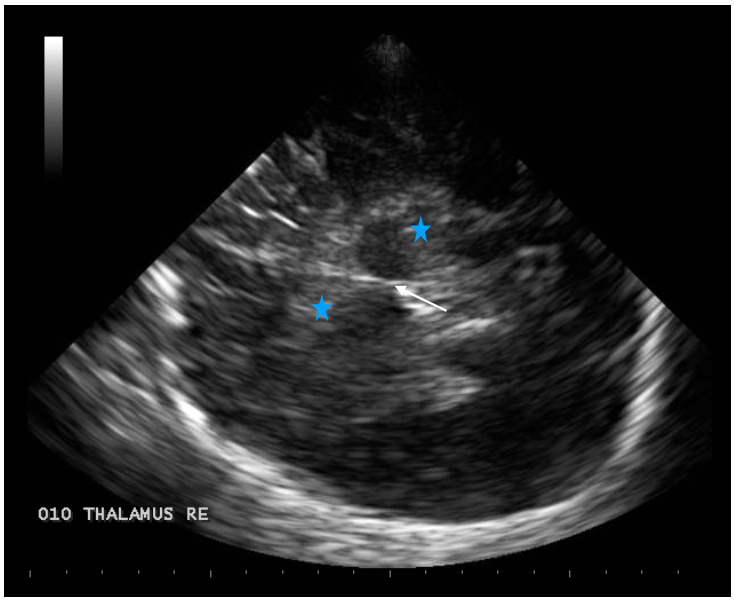

Figure 2.3: Diencephalon plane: bilateral thalamus is indicated by the blue stars, arrow points to third ventricle.

2.4 Magnetic Resonance Imaging

For MRI a 3 - Tesla Magnetom Trio Scanner (Siemens, Erlangen, Germany) was deployed. T_1-weighted turbo field echo (TFE) sequences were used for neuromelanin-sensitive MR image acquisition with the following parameters: repetition time (TR): 600 ms, echo time (TE): 10 ms, field of view (FoV): 178 x 220 mm, matrix size: 416 x 512, in plane (pixel) resolution: .43 x .43 mm, slice thickness: 2.5 mm, 4 x 2 averaged, and a total acquisition time of 16 : 32 min. In addition, anatomical T_1- MRI sequences were obtained and examined to exclude pathological imaging findings. Magnetization prepared rapid gradient echo (MPRAGE) sequences were applied with 176 slices, TR: 2300 ms, TE: 2.95 ms, FoV: 270 mm, flip angle 9°, slice thickness: 1.2 mm. One participant refused MRI measurement.

2.5 Serum Iron Parameters

To assess peripheral iron levels, venous blood samples were taken. A total of 29 participants delivered blood samples. Five subjects refused a venepuncture due to vegetative symptoms such as nausea or due to personal reasons. Blood samples were analyzed for the following parameters that are related to iron metabolism: iron, ferritin, transferrin, transferrin saturation (TSAT) and C-reactive protein (CRP). Analyses were done in the central laboratory of Wuerzburg University Hospital.

Iron: Serum iron concentration varies strongly during the day. It depends on food intake and circadian rhythms. High levels can indicate hemochromatosis or hemolytic anaemia. Low levels can be due to increased requirements (e.g. pregnancy), iron loss (e.g. hemorrhage), inadequate supply (e.g. vegetarianism) or insufficient absorption (Dörner, 2009). Reference intervals for children ($2 - 14$ $years$) ranged from $80 - 165$ $\mu g/dl$.

Ferritin: Ferritin is a protein and the main intracellular storage of iron. It is also released to some degree into blood plasma. This concentration correlates with intracellular ferritin. Therefore, it can be used as indirect marker for

the total amount of stored iron. Ferritin is high in iron excess and acute inflammatory reactions. It is low during iron deficiency. Ferritin is also an acute-phase protein. Infections can trigger high ferritin concentrations and thereby mask underlying low concentrations (Dörner, 2009). Reference intervals for children $1 - 12\ years$ were: $9.3 - 59\ \mu g/l$.

Transferrin: Transferrin is a glycoprotein that binds to iron and serves as the main transport mechanism for cellular iron uptake. During iron deficiency transferrin concentration is reactively high. On the other hand it is low in iron overload diseases and during acute-phase (Dörner, 2009). Reference intervals for children ranged from $215 - 360\ mg/dl$.

TSAT: TSAT indicates saturation of transferrin proteins with iron.

$$TSAT(\%) = 70.9 \times \frac{serum\ iron\ (\mu g/dl)}{serum\ transferrin\ (mg/dl)}$$

Rates are high in iron overload and low in iron deficiency (Dörner, 2009). Reference intervals for children extended from $15 - 45\ \%$.

CRP: CRP is produced in the liver and functions as an acute-phase parameter, it is a marker for acute infections (Dörner, 2009). Since iron levels can also be altered due to infections, CRP was quantified in addition. Thereby facilitating the distinction of acute infections and chronic changes in iron metabolism. None of the blood samples reached the clinical cut-off scores of $.5 mg/dl$, making a severe acute infection rather unlikely.

2.6 Procedure

Participants and their legal guardians were again informed about course, timing and purpose of this study. Written informed consent was obtained. Claustrophobia, metal implants and pacemaker were again explicitly inquired and excluded. The procedure had a total duration of approximately 1 hour for each subject. All participants ran through the following 3 measurements but they were free to choose if they wanted to start with TCS or MRI.

1. TCS: TCS image collection took about 15 minutes for each subject. Participants were lying supine, the examiner sitting behind their head. The ultrasound probe was pressed firmly to the preauricular region, angling the probe in parallel towards an imagined orbitomeatal line. Images of all planes were obtained gradually by tilting the probe on each side of the head systematically. The procedure was repeated for left and right sides of the head respectively.

2. MRI: MRI data acquisition required approximately 35 minutes for each subject. Participants were asked to lay still and relax in order to reduce artifacts. In addition, the head was stabilized using a headrest with side pads. To further support their compliance and minimize motion artifacts, subjects could choose to watch a children's film.

3. Bloodsample: To reduce stress and anxiety due to venepuncture, blood samples were taken at the end of the whole experiment. The procedure lasted about 10 minutes. After local disinfection, a serum tube for each subject was taken from vena mediana cubiti.

2.7 Data Analysis

2.7.1 MRI

Matlab (R2010a, The MathWorks, Natick, Massachusetts, USA) was used for preprocessing of MRI data. In order to improve the signal-to-noise ratio, noise reduction and spatial smoothening with a Gaussian filter $2\ mm\ x\ 2\ mm$ were performed. Subsequently, volumetric SN data and signal intensity measures of SN were derived from MRI data. Signal intensity and SN volume were measured semi-automatically with a modified version of Perfusion Mismatch Analyzer, version 5.0.5.5 (©Kudo, 2006) that has been used before accordingly (Ogisu et al., 2013). Using a circular region of interest (ROI) of 6 mm in diameter, signal intensity of the decussatio of the superior peduncle of the cerebellum was determined with Perfusion Mismatch Analyzer. Each signal intensity of the substantia nigra was then standardized against the signal intensity of the ROI in the superior peduncle of the cerebellum, thereby cancelling out differences in overall signal intensity among subjects. SN volume was calculated semi-automatically by statistically comparing intensity measures of seed-points in high intensity areas (corresponding to the SN) relative to a threshold that derived from signal intensity in the cerebellar ROI. The statistically significant suprathreshold voxels automatically configured SN neuromelanin volume. In addition, contrast ratios were computed to extract and quantify signal intensity of the neuromelanin signal (Sasaki et al., 2006).

$$Contrast\ Ratio\ SN = \frac{(signal\ intensity\ substantia\ nigra) - (signal\ intensity\ cerebellar\ peduncle)}{(signal\ intensity\ cerebellar\ peduncle)}$$

2.7.2 TCS

Except for reliability assessment and data exploration, in all analyses the maximum *SN echogenic size* (thus the largest measurement of each bilateral measurement) was used (Walter, 2012). Three participants had no sufficient left temporal acoustic bone windows, here right hemispheric data were used. Hyperechogenicity was determined according to standard recommendations as $\geq 75\,percentile$. Pronounced hyperechogenicity was defined as signal extensions $\geq 90\,percentile$ (Walter et al., 2007).

2.7.3 Statistical Analysis

Analyses were run using SPSS 23 and SPSS 25 (SPSS Statistics, IBM, Germany) and two-tailed significance tests ($p < .05$) are reported. Descriptive statistics are given as $mean$, standard deviation (SD) and $minimum - maximum$. Outliers were detected by visual inspection of box blots or estimated by $z - scores$. Data were analyzed by Shapiro-Wilk tests to test for normality. In small sample sizes Shapiro-Wilk is preferable as it has more power. For parametric data, Pearson correlation was used to determine association between two variables. For nonparametric data, Spearman's rho correlation coefficients were calculated. Bivariate correlations were considered to investigate the association of SN echogenicity with the different SDQ subscales. A series of separate linear regression models were deployed to assess the relation between SN echogenicity and central MRT neuromelanin data as well as SN echogenicity and peripheral serum iron parameters. To discern possible interaction effects, regression analyses with moderator models were performed using PROCESS, version 3.1 (©Hayes, 2012) a free software macro i.a. for SPSS. Model 1 with 10000 bootstrap iterations and heteroscedasticity-consistent standard error estimators (HC3, Davidson-MacKinnon) was employed. Bootstrapping is a resampling method to estimate population parameters. By constructing a number of bootstrap resamples (with replacement) of the primary data sample, the parameter distribution of the population can be approximated and modeled by the empirical parameter distribution. The default use of heteroscedasticity-consistent standard error estimators has been recommended in linear regression models (Hayes & Cai,

2007). Durbin-Watson test was used to check for independent errors. Normal probability plots and Shapiro-Wilk tests of the residuals were evaluated to ensure normally distributed errors. Potential multicollinearity was examined by correlation matrices and VIF. Standardized residuals and predicted values helped to rule out heteroscedasticity. Influential cases were assessed by Cook's distance, leverage values and standardized DFBeta values. To test for differences between groups Mann-Whitney test (2 groups) was used for nonparametric data, it is based on ranked data and $exact\ p$ is reported. Lines-of-best-fit (least square method) are used to illustrate correlations. Andy Field's "Discovering Statistics Using SPSS" (2005) helped to answer specific statistical questions and understand settings in SPSS routines.

3 Results

A total of 6 subjects had to be excluded from final data analyses due to: insufficient bone window (1 case), conspicuous $SDQ = 93\,\%ile$ (1 case) or female gender (4 cases). Since gender has been shown previously to have an effect on SN echogenicity (Schweitzer et al., 2007) and also movement disorders are more prevalent among man (Loke, Harley & Lee, 2015) only male participants were finally included, leaving a total of 28 participants.

From those subjects finally included in further analyses, datapoints were missing for 1 subject who rejected MRI scan. Three subjects refused venipuncture. Due to technical problems in the laboratory for 3 subjects parts of the blood parameters were missing. Cases were excluded listwise.

3.1 Descriptives and Characteristics

Descriptive statistics and frequency tables for several subject characteristics and serum parameters are given in table 1. $Mean$ age was 9.8 years ($SD = .95$) and mean IQ was 111.6 ($SD = 14.83$).

Descriptive Statistics

	N	Minimum	Maximum	Mean	Std. Deviation
Age	28	8	12	9.82	.945
IQ	28	86	144	111.61	14.831
Iron (µg/dl)	22	47	142	93.59	23.826
Ferritin (µg/l)	25	23	135	60.12	35.359
Transferrin (mg/dl)	25	212	306	259.56	24.818
TSAT (%)	22	10.9	47.5	26.123	8.163
CRP (mg/dl)	25	0	.36	.032	.076

Table 1: Descriptive statistics of age, IQ and iron-related serum measures.

Blood parameters were additionally rated according to age-related norms to

indicate if they were below norm, within norm or above norm. Within the scope of normal measuring inaccuracy, subjects mostly had only minor abnormalities in 1 parameter. Serum iron was below norm in 5 subjects, none had a surplus. Ferritin was above norm in 9 subjects. None of the children showed ferritin concentrations below norm. Although unfortunately further information on e.g. hemoglobin, reticulocytes was not obtained, iron deficiency anemia is improbable. Transferrin was below norm in 1 subject, no serum concentrations were above reference intervals. TSAT was deficient in 2 subjects and above norm in 1 subject. Two children had a low TSAT and low iron indicating a slight iron undersupply, but their ferritin was within normal range. Serious infections mostly involve elevated CRP. In this sample CRP was within norm for all subjects.

Boxplots (figure 3.1) and a separate table (2) display descriptive statistics of SDQ and its subscales. Total SDQ was within a range from $50 - 90th\ percentile$ with $mean = 59.86\ percentile$. Interpretation of the results in terms of deviation from the norm ($\gtrsim 80\ percentile = borderline\ or \gtrsim 90\ percentile = conspicuous$) showed that 3 children had more emotional problems than the norm, 3 had abnormal high ratings on conduct problems, 1 subject was above normal reference values on hyperactive behavior, 1 had upper scale scores on problems with peers and 6 children showed less prosocial behavior than normal reference values suggest. Note, as opposed to the other scales, in prosocial behavior lower values (≤ 20) indicate deviations from the norm. $Conspicuous$ total SDQ was an exclusion criterion, therefore only 2 $borderline$ values were contained within the final data (90 & $87\ percentiles$).

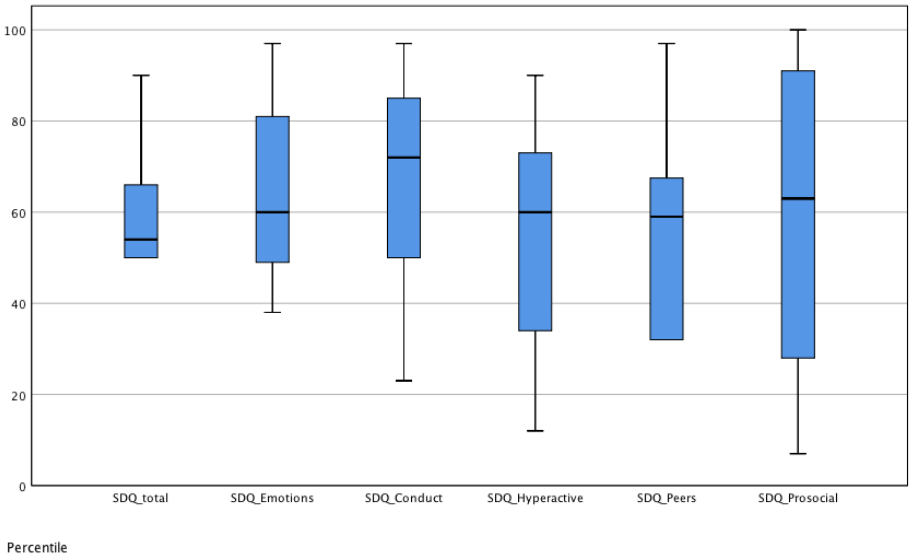

Figure 3.1: Boxplots for distribution of total SDQ and SDQ subscales (emotional problems, conduct problems, hyperactivity, problems with peers and prosocial behavior) in $percentile$. $Median$ is indicated by the line, whiskers mark upper and lower $quartiles$, box represents $interquartile\ range$.

Descriptive Statistics

	N	Minimum	Maximum	Mean	Std. Deviation
SDQ_total (%ile)	28	50	90	59.86	12.704
SDQ Emotions (%ile)	28	38	97	64.89	19.689
SDQ Conduct (%ile)	28	23	97	64.54	22.088
SDQ Hyperactivity (%ile)	28	12	90	52.14	25.824
SDQ Peers (%ile)	28	32	97	52.82	20.505
SDQ Prosocial (%ile)	28	7	100	57.93	33.547

Table 2: Descriptives for total SDQ and SDQ subscales (emotional problems, conduct problems, hyperactivity, problems with peers and prosocial behavior).

Neuroimaging of the substantia nigra was conducted with TCS and MRI. $Means$, SD and $minimum - maximum$ are described in table 3 and data points of each subject are illustrated in figure 3.2. In TCS, measurements of the individual hemispheres showed corresponding values. $Mean$ size of right SN echogenic area

was .104 cm^2, $SD = .043$ and $mean$ left SN echogenic area was .104 cm^2, $SD = .038$. Volumetric data from MRI had a $mean$ of .167 cm^3, $SD = .033$ and $mean$ neuromelanin contrast was $5,8\,\%$, $SD = .044$. In 2 nine-year old participants contrasts were negative ($-1,6\,\%$ & $-1,1\,\%$) and accordingly neuromelanin volume of the SN was relatively small (.130 cm^3) in both subjects. If not due to noise or measuring inaccuracy, in young children low neuromelanin signals can be reasonable. Diminished signals fit with theoretical and empirical considerations, which state that nigral neuromelanin first starts to accumulate around the age of 3 and that the SN subsequently slowly increases in neuromelanin content with age.

Furthermore, to examine gross signal abnormalities in TCS contralateral thalamus and ventricle width were evaluated. All subjects showed normal thalamus echogenicity. None of the subjects showed ventricle widths over $4.9\ mm$ ($min - max = .9 - 4.9$). This is far below adult cut-off scores and in the absence of reference values for children this was accepted.

Descriptive Statistics

	N	Minimum	Maximum	Mean	Std. Deviation
TCS SN right (cm^2)	28	.032	.210	.104	.043
TCS SN left (cm^2)	25	.050	.189	.104	.038
TCS SN (cm^2)	28	.043	.210	.112	.042
SN Volume (cm^3)	27	.10	.22	.167	.033
Contrast_SN	27	-.016	.161	.058	.044

Table 3: Descriptives for signal measurements of substantia nigra with TCS and MRI. TCS SN right refers to right SN sizes in cm^2, TCS SN left denotes left SN size in cm^2, TCS SN is composed of the maximum value of each bilateral assessment in cm^2. SN Volume shows volumetric SN values in cm^3 from neuromelanin-sensitive MRI measures, Contrast_SN refers to SN neuromelanin contrasts obtained with MRI.

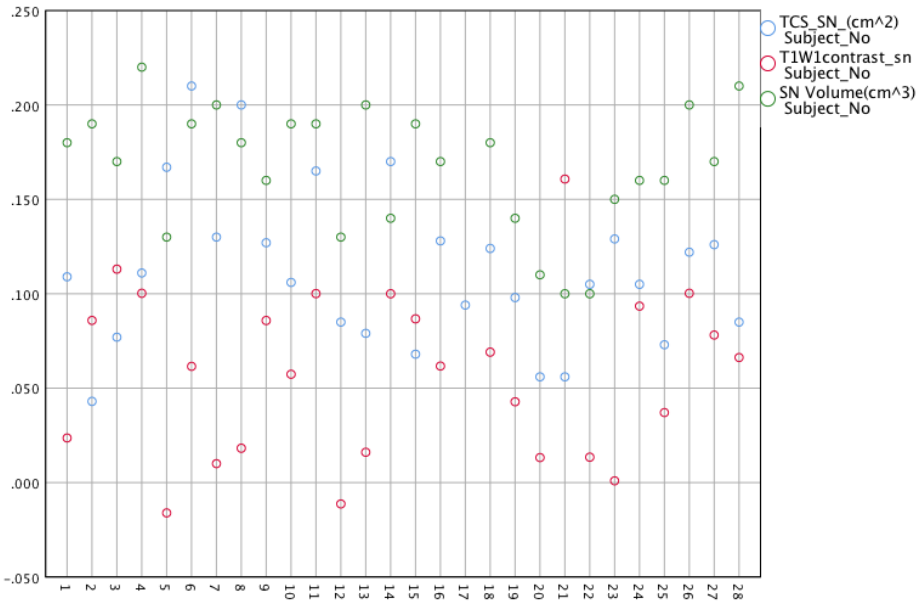

Figure 3.2: Neuroimaging measures of the SN of each subject. X-axis displays serially numbered subjects. Neuroimaging data (y-axis) of TCS (blue dots), MRI neuromelanin volume (green dots) and neuromelanin contrasts (red dots) are plotted in distinct colors, each data point corresponds to an individual measurement.

3.2 Reliability Assessment of TCS Measures

In order to check for reliability and agreement among TCS measures the following statistics were made. Pearson correlation between *left* ($mean = .104\,cm^2$, $SD = .038$) and *right* ($mean = .104\ cm^2$, $SD = .043$) side TCS measures of SN was good $r = .781$, $p < .000$, suggesting congruity of the two sides and reliable, consistent measures (see Figure 3.3). $Mean$ diameter of the third ventricle was .191 cm, $SD = .069$ when TCS was executed on the *right side,* and .201 cm, $SD = .082$ for *left side* measures. Spearman's rho between the two assessment sides was high $r = .888$, $p < .000$.

To validate TCS measurements and further assess their reliability, SN measurements were additionally independently evaluated by two examiners (J.G. and L.S.). Inter-rater reliability was calculated using Kendall's W. Kendall's W is a non-parametric measure for agreement amongst multiple (> 2) raters if variables are continuous. Kendall's W takes values between $0 - 1$, higher values indicating higher concordance. Here, the coefficient of concordance displayed moderately high concordances between the 3 examiners, $\text{Kendall's } W = .717$, $p \leq .05$.

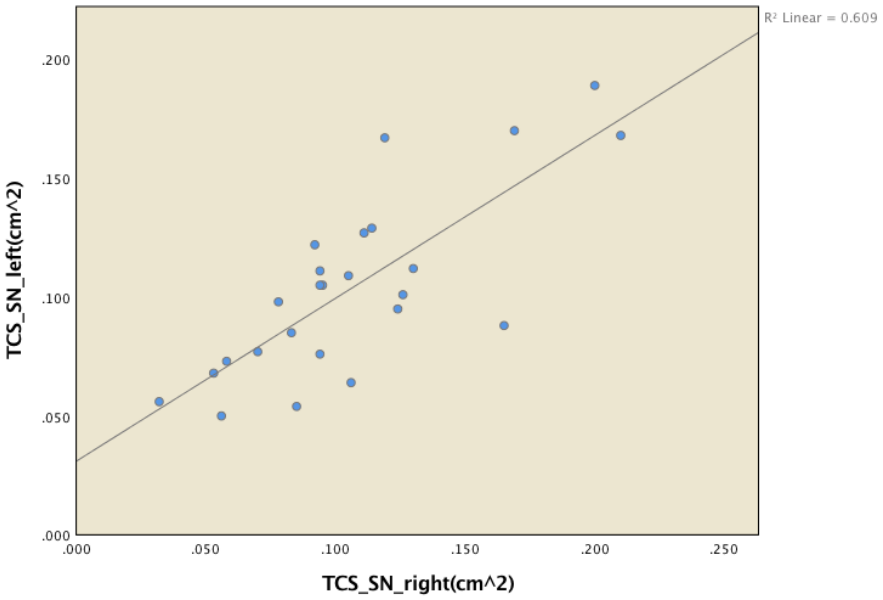

Figure 3.3: Scatterplot for *left* (y-axis) and *right* (x-axis) SN measures (in cm^2) with line-of-best-fit. Pearson correlation was significant $r = .781$, $p < .000$.

3.3 Substantia Nigra Echogenicity in Healthy Children

For further analyses the larger SN area of each left and right measurement was chosen and hereafter termed *SN echogenic size*.

Mean SN echogenic size was then .112 cm^2 ($SD = .042, min - max = .043 - .210\, cm^2$). Figure 3.4 displays the distribution of individual measurements. Shapiro - Wilk test ($= .955, p = .267$) confirms normal distribution. Pearson correlation did not show a significant correlation between *IQ* and *SN echogenic size* (cm^2) ($r = .094, p = .634$).

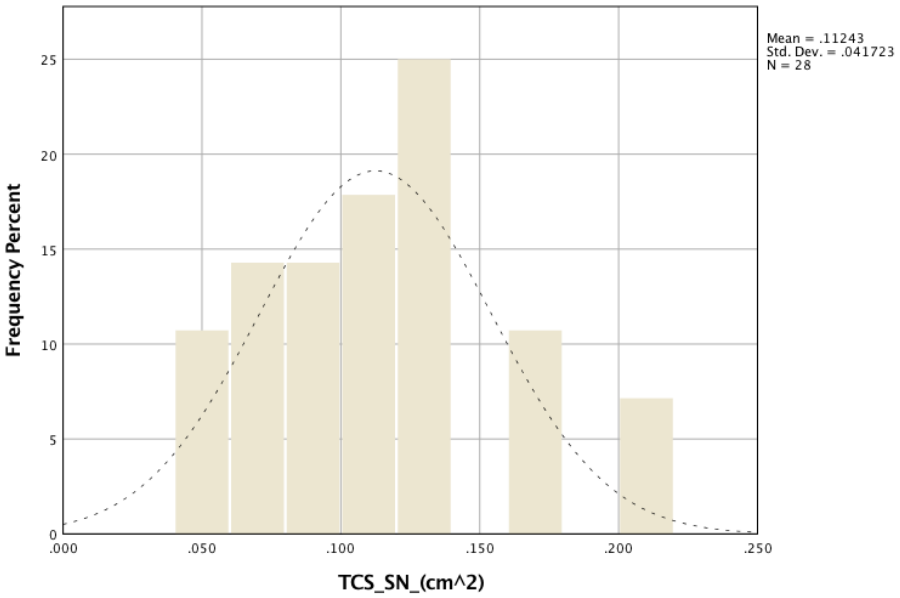

Figure 3.4: Distribution of *SN echogenic size* in cm^2 as a function of its frequency (%).

In this healthy children sample normoechogenic SN sizes ranged from $.043 - .127\ cm^2$ with $mean = .092\ cm^2 (SD = .025)$. Hyperechogenicity was determined as SN sizes of $\geq .128\ cm^2$ ($\geq 75\ percentile$) and pronounced hyperechogenicity as $\geq .173\ cm^2$ ($\geq 90\ percentile$). Boxplots for visualiza-

tion are given in figure 3.5. Thus, hyperechogenic SN varied between sizes of $.128 - .172\ cm^2$ with $mean = .144\ cm^2$ ($SD = .020$) and pronounced hyperechogenicity between $.173 - .210\ cm^2$ with $mean = .193\ cm^2$ ($SD = .021$).

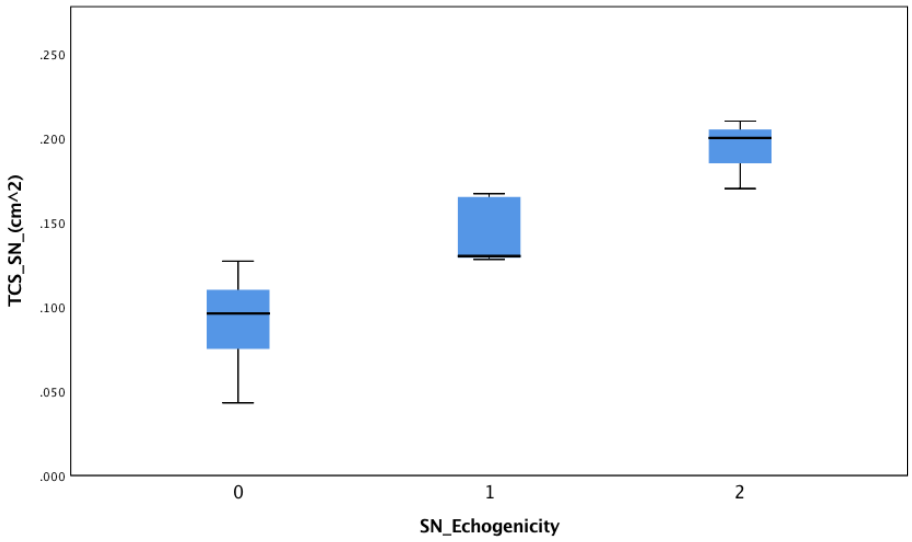

Figure 3.5: Boxplot illustrates normoechogenic (0), hyperechogenic (1) and pronounced hyperechogenic (2) SN echogenicity in cm^2. Shown are $median$, $25\ and\ 75\ percentile$ and $interquartile\ range$ represented by the box.

3.4 Substantia Nigra Echogenicity and Behavioral Ratings

SN echogenic size (cm^2) correlated significantly with *SDQ Hyperactivity* ($percentile$) (Spearman's rho $r = -.602, p = .001$). The relationship was inverse: healthy children with more extended SN sizes showed less hyperactive behavior than those with less extended SN echogenic signals (figure 3.6).

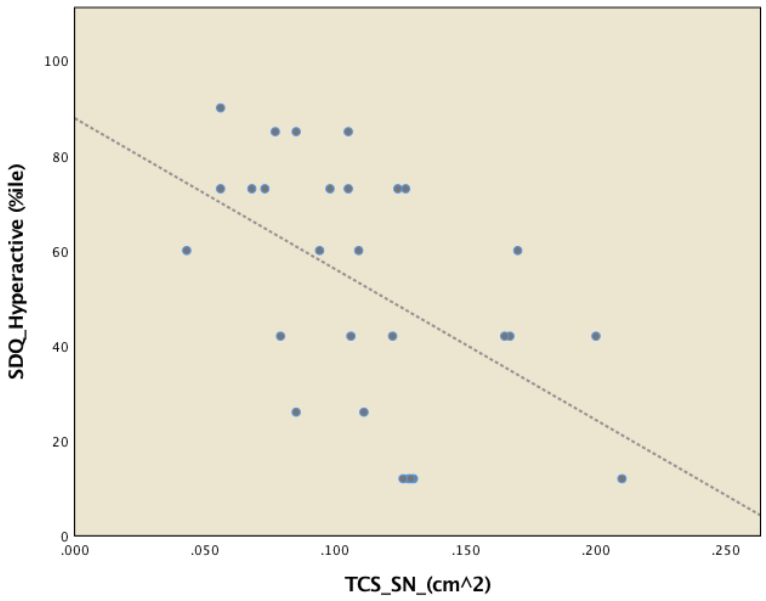

Figure 3.6: Scatterplot with line-of-best-fit displays the association of SN echogenicity (cm^2) and hyperactive behavior ($percentile$): more hyperactive behavior is related to less SN echogenicity. Correlation was significant (Spearman's rho $r = -.602, p = .001$).

Differences in *SDQ Hyperactivity* ($percentile$) between *normoechogenic* and *hyperechogenic SN* were were significant. Boxplots in figure 3.7 illustrate the $median\ percentile$ (group 0 = 73.000; group 1 = 27.000) and differences in *SDQ Hyperactivity* ($percentile$). Mann-Whitney test on differences in *SDQ Hyperactivity* ($percentile$) between the *echogenic groups* showed significant differences ($U = 23.000$, $exact\ p = .002$). In healthy children, children

with normoechogenic SN exhibit more hyperactive behavior than children with hyperechogenic SN. Data were assessed to gain preliminary evidence about SN hyperechogenicity as a structural marker for functional differences in healthy children. Overall sample size and hence N in the different groups was small: *normoechogenic SN* ($\leq .127\ cm^2, N = 20$), *hyperechogenic SN* ($\geq .128\ cm^2, N = 8$). Therefore the data have to be considered to be rather explorative.

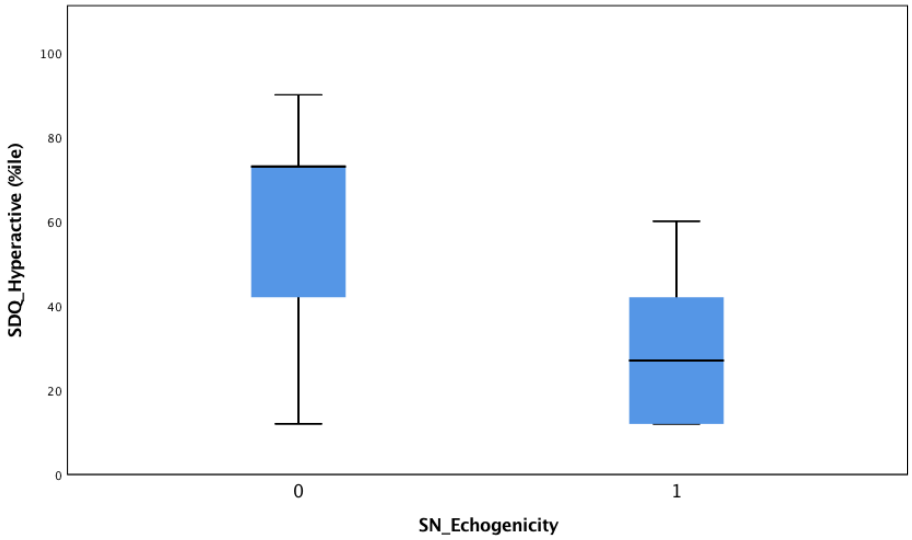

Figure 3.7: Differences in *SDQ Hyperactivity* ($percentile$) for subjects with *normoechogenic* (0) and *hyperechogenic* (1) SN. Shown are $median$, $25\ and\ 75\ percentile$ and $interquartile\ range$ represented by the box. $Mean$ *SDQ Hyperactivity* in group 0 was 61 $percentile$, ($SD = 22.375$) and in group 1 $mean$ *SDQ Hyperactivity* lied at 29 $percentile$, ($SD = 19.359$). Differences in *SDQ Hyperactivity* between children with *normoechogenic* and *hyperechogenic SN* were significant ($exact\ p = .002$).

SN echogenic size (cm^2) did not correlate with SDQ scales for emotional problems *SDQ Emotions* (Spearman's rho $r = -.006, p = .976$), problems with peers *SDQ Peers* (Spearman's rho $r = -.288, p = .138$) and prosocial behavior *SDQ Prosocial* (Spearman's rho $r = .223, p = .255$). But a significant correlation was found between *SN echogenic size* (cm^2) and conduct problems *SDQ Conduct* ($percentile$) (Spearman's rho $r = -.387, p = .042$). Children having more extended SN sizes showed less conduct problems than those with smaller SN echogenic signals (figure 3.8). In addition, intercorrelation of *SDQ Hyperactivity x SDQ Conduct* (Spearman's rho $r = .403, p = .033$) was significant.

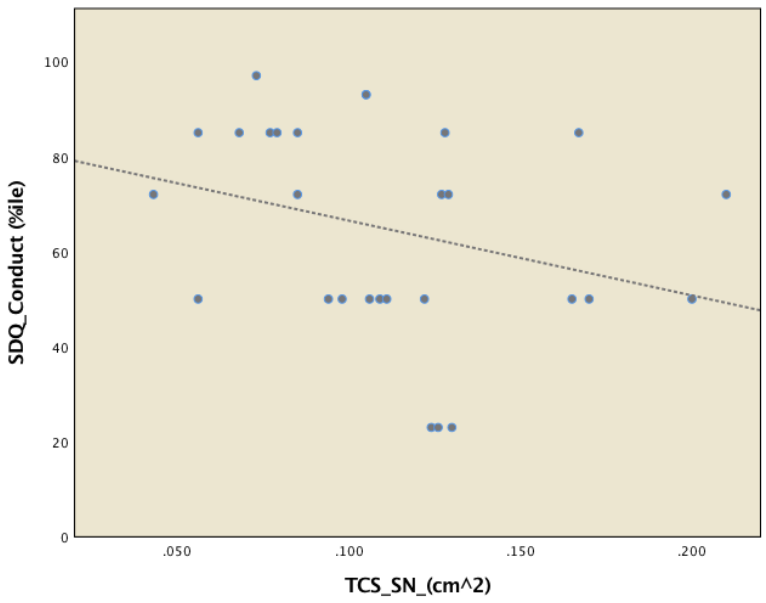

Figure 3.8: Scatterplot with line-of-best-fit for SN echogenicity (cm^2) and SDQ conduct problems ($percentile$). Non-parametric correlation was significant (Spearman's rho $r = -.387, p = .042$).

Since more hyperactive behavior in ADHD has repeatedly been related to lower peripheral ferritin levels, their association was also assessed in the present sample.

SDQ Hyperactivity ($percentile$) did not correlate with *ferritin (µg/l)* (Spearman's rho $r = -.026, p = .900$). Also none of the subscales changed as a function of *age: SDQ Hyperactivity x age* (Spearman's rho $r = -.129, p = .513$), *SDQ Conduct x age* (Spearman's rho $r = -.111, p = .576$), *SDQ Emotions x age* (Spearman's rho $r = -.089, p = .653$), *SDQ Prosocial x age* (Spearman's rho $r = .060, p = .761$), *SDQ Peers x age* (Spearman's rho $r = -.048, p = .807$).

3.5 Regression Analyses

Regression Analyses Peripheral Iron Status There was no significant association between peripheral iron levels and SN echogenicity. Regression models with *iron x ferritin x transferrin x TSAT* did not predict *SN echogenic size* (cm^2). Stepwise backwards methods were used, predictors that failed to improve the model were successively eliminated. Results are outlined in table 4. Due to the nature of *TSAT*, potential multicollinearity with *iron* and *transferrin* could not be ruled out and a separate model for *TSAT* was analyzed (model 4). For an overview of all preliminary correlations see matrix table 8 in the appendix.

Model		B	SE B	β	t	p
1	Constant	.124	.150		.826	.420
	Ferritin (µg/l)	.000	.000	-.322	-1.375	.186
	Iron (µg/dl)	.000	.000	.106	.410	.687
	Transferrin (mg/dl)	.000	.000	-.011	-.043	.966
2	Constant	.118	.040		2.939	.008
	Ferritin (µg/l)	.000	.000	-.320	-1.438	.167
	Iron (µg/dl)	.000	.000	.111	.499	.624
3	Constant	.135	.018		7.462	.000
	Ferritin (µg/l)	.000	.000	-.297	-1.389	.180
4	Constant	.123	.033		3.677	.002
	Ferritin (µg/l)	.000	.000	-.323	-1.429	.169
	TSAT (%)	.001	.001	.100	.442	.663

Table 4: Stepwise backwards regression analysis. Regression parameters of the models involving peripheral iron parameters. B, $standard\,error\,(B), \beta, t$, $p-values$ are given. None of these models and variables could significantly predict SN echogenicity. $R^2 = .100, F = .666, p = .584$ (model 1), $R^2 = .100, F = 1.053, p = .368$ (model 2), $R^2 = .088, F = 1.929, p = .180$ (model 3), $R^2 = .097, F = 1.024, p = .378$ (model 4).

Regression Analyses Central Neuromelanin Data Separate hierarchical models were conducted in order to assess if nigral neuromelanin data can predict nigral TCS signals. Regression analyses with *SN Volume* (cm^3) *x Contrast_*SN did not reveal any significant models or associations between TCS measures and MRI data of the SN in this sample. Neither neuromelanin signal intensity ($\beta = -.213, p = .296$), nor SN neuromelanin volume ($\beta = .213, p = .296$) could predict *SN echogenic size* (cm^2) in meaningful models (table 5). Also if the effect of the respective other variable was held constant, there was no evidence that *SN echogenic size* (cm^2) was significantly related to *Contrast_*SN ($\beta = -.272, p = .188$) and *SN Volume* (cm^3) ($\beta = .272, p = .188$). Thus, variance in *SN echogenic size* could not be significantly explained. Table 5 subsumes all regression results. Correlation between the 2 neuromelanin-related MRI predictors *SN Volume x Contrast_*SN was not significant ($r = .217$, $p = .143$) and diagnostics did not indicate serious collinearity ($VIF = 1.05, Tolerance = .95$).

Model		B	SE B	β	t	p
1	Constant	.066	.043		1.526	.140
	SN Volume (cm^3)	.269	.252	.213	1.069	.296
2	Constant	.122	.013		9.112	.000
	Contrast_SN	-.202	.189	-.213	-1.069	.296
3	Constant	.068	.042		1.600	.123
	SN Volume (cm^3)	.343	.253	.272	1.356	.188
	Contrast_SN	-.258	.190	-.272	-1.356	.188

Table 5: Coefficients (B, $standard error(B)$, β, t, $p-values$) of the regression models for SN echogenicity with neuromelanin-related MRI data. Model 1: $R^2 = .045, F = 1.143, p = .296$. Model 2: $R^2 = .045, F = 1.142, p = .296$. Model 3: $R^2 = .116, F = 1.510, p = .242$.

Regression Analyses Age To assess possible developmental aspects, regression analyses with *age (years)* were performed to investigate if *age (years)* of the children can predict their *SN echogenic size* (cm^2). In this sample, age could not predict SN echogenic size. There was no significant relation ($\beta = .303$, $p = .117$) between *age (years)* and *SN echogenic size* (cm^2). It was furthermore examined if the relationship between *SN echogenic size* (cm^2) and the neuromelanin MRI data *SN Volume* (cm^3), *Contrast_*SN was moderated by *age (years)*. Moderation analysis with *age* as moderator did not reveal a significant interaction of $age * Contrast\ SN$ ($B = .102$, $p = .769$) or a statistically relevant interaction of $age * SN\ Volume$ ($B = .068$, $p = .889$). Also main effects were not significant, detailed results are given in table 6. Correlation matrix is listed in table 7 in the appendix. Hence, within this sample nigral echogenic signals could not be predicted by neuromelanin data and age, besides their relation was not moderated by the age of the children.

Model		B	SE B	β	t	p
1	Constant	-.019	.081		-.231	.819
	Age	.013	.008	.303	1.619	.117
2	Constant	.110	.010		11.081	.000
	Contrast_SN	-.278	.266		-1.045	.308
	Age	.016	.014		1.109	.279
	Age*Contrast_SN	.102	.343		.298	.769
3	Constant	.110	.009		12.473	.000
	SN Volume (cm^3)	.185	.282		.657	.518
	Age	.010	.012		.855	.402
	Age*SN Volume	.068	.484		.141	.889

Table 6: Regression analyses and moderation models with *age* and MRI neuromelanin parameters as predictors for *SN echogenic size* were not significant. Interaction terms are denoted by $age * Contrast\ SN$ and $age * SN\ Volume$. Model 1 ($R^2 = .092, F = 2.621, p = .117$), model 2 ($R^2 = .197, F = .957, p = .430$), model 3 ($R^2 = .107, F = .488, p = .694$).

4 Discussion

TCS has proven to be a useful, inexpensive and flexible tool in the assessment of movement disorders. Yet there are very few publications on TCS of the SN in children. The purpose of this study was to help establish reference values of the SN in healthy children and to relate SN echogenicity to subclinical alterations in behavior. Furthermore, associations of peripheral serum iron parameters and central nigral neuromelanin measures to TCS signals of the SN were evaluated. And moreover, the question was addressed if neuroimaging signals of the SN show age-related changes.

In adults SN sizes equal to or greater $.20\ cm^2$ are considered to be hyperechogenic and sizes of $.25\ cm^2$ and above are labeled as markedly hyperechogenic (Walter et al., 2007). Hyperechogenicity is not only found in movement disorders but also in about 10% of healthy adults (Berg et al., 1999a; Schweitzer et al., 2007). In children hitherto inconclusive values have been reported. To help establish reference values for children, SN echogenicity was determined according to common guidelines. In this sample, hyperechogenic SN in healthy children extended from $.128 - .210\ cm^2$ and pronounced hyperechogenicity from $.173 - .210\ cm^2$. Those sizes approximate echogenic sizes of ADHD children (Romanos et al., 2010), hyperechogenic sizes in another data set of healthy children (Iova et al., 2004) as well as sizes of adults (Walter et al., 2007). Normoechogenicity varied between $.043 - .127\ cm^2$.

Nowadays it is widely acknowledged that behaviors exhibit a flowing continuum from adaptive to non-adaptive and consequently some disorders, amongst others ADHD, should be seen as as dimensional rather than categorical (Coghill & Sonuga-Barke, 2012; Marcus & Barry, 2011). Hence, even if manners are not clinically relevant or pathological, certain phenotypes and differences still exist. In healthy adults there is evidence that SN hyperechogenicity is associated with subclinical alterations in behavior and PD-like symptoms such as motor slowing (Berg et al., 2001b). In an attempt to link SN echogenicity to subclinical behavioral

tendencies in healthy children, behavioral screening questionnaires were obtained. As expected there was a significant association between hyperactivity ratings and SN echogenicity and no statistically relevant association with emotional problems, prosocial behavior or problems with peers. Contrary to expectations, SN echogenicity was inversely related to hyperactivity ratings in healthy, non-ADHD children. Children with higher nigral echogenicity showed less "hyperactive" behavior. In other words, hyperactive tendencies were associated with low SN echogenicity. To date there is no clear-cut definition of subclinical and subthreshold forms of ADHD. However, there is substantial evidence that it is a risk factor and that comorbidities of substance abuse, oppositional defiant disorder, conduct disorder, major depression disorder and others are frequent. Moreover, it is a common condition, point prevalences range from $1-23\%$ (for a systematic review see: Balázs & Keresztény, 2014). Preventive strategies, thorough attention and early interventions may be crucial for children who are at risk of subthreshold ADHD and an echogenic marker could help to identify those children at risk. If confirmed in future studies, nigral echogenicity might be useful also in the assessment of subclinical forms of ADHD.

The findings are intriguing. Nevertheless, the investigation was based on questionnaires and no actual behavioral data were gathered. Further limiting was the exclusive use of parental rating scales and additional external information e.g. from teachers would increase the accuracy of their ratings. It has been shown that teachers have more elaborate diagnostic observational skills when it comes to ADHD rating scales (Kóbor et al., 2012). Besides, while giving a good overview about the overall psychological phenotype and good reliability & validity with other scales, SDQ consists of only 5 hyperactivity items. A more extensive questionnaire on hyperactivity would conduce to augment the concept and importantly also allow for the discrimination of the different ADHD subtypes resp. dimensions. Due to the brief and compact questionnaire, discrimination in the present study was not reasonable.

In the current study, children with less SN echogenicity showed more hyperactive behavior. Continuing preliminary analyses revealed that children with hyperechogenic SN exhibited indeed significantly less hyperactive behavior than those with normoechogenic SN. Although, the latter results are rather explorative,

sample sizes were small and outcomes have to be replicated in studies with more power. In adults SN hyperechogenicity is considered to be a marker for nigrostriatal vulnerability and it is associated with reduced dopaminergic uptake in the striatum (Behnke et al., 2009; Berg et al., 1999a, 2002). Functional considerations of echogenic alterations in healthy and ADHD children have not yet been enlightened. However, if hyperechogenicity in healthy children also reflects dopaminergic dysfunction, in the present study there is no evidence that it is associated with reports of more hyperactive behavioral tendencies. Thus, the question remains if those children with nigral hyperechogenicity show other subclinical symptoms of dopaminergic disruption.

In the past, upwards and downwards deviations in nigral echogenic sizes have been associated with certain phenotypes: hypoechogenicity is found in RLS (Godau & Sojer, 2010; Schmidauer et al., 2005) and hyperechogenicity in PD (e.g. Becker et al., 1995; Berg et al., 2008) and ADHD (Krauel et al., 2010; Romanos et al., 2010). There is no clear consensus on the definition and measurement requirements of hypoechogenicity (Skoloudík & Walter, 2010) and in the current study it has not been further investigated. Nevertheless, the difference in hyperactive behavior might actually narrow down to a difference between hypoechogenic and hyperechogenic SN. Although to date this remains speculation and needs investigation in further studies.

SN echogenicity also correlated significantly with scales on conduct problems. Again the relation was inverse, children with higher SN echogenicity had lower scores in conduct problems and vice versa. The correlation was rather weak. Nevertheless, SN echogenicity has been related to conduct problems in ADHD children before: ADHD children with hyperechogenic SN had significantly lower symptoms of oppositional defiant disorder than children with normoechogenic SN (Krauel et al., 2010). The authors at that time argued, that there is evidence for a special ADHD subtype with oppositional defiant disorder/conduct disorder. In any case, comorbidity of ADHD and oppositional defiant disorder or conduct disorder is well known (e.g. Loeber et al., 2000; Noordermeer et al., 2017). The interconnection seems to hold also true for behavioral tendencies in healthy children, here in this sample hyperactivity ratings and conduct problems were significantly positively correlated.

Evidence suggests that aberrant free iron deposits and altered iron-handling, such as neuromelanin, are involved in the biophysics which underlie SN hyperechogenic signals (Berg et al., 1999b, Zecca et al., 2005). Neuromelanin binds iron, is contained in catecholaminergic neurons in the SN and supposedly has a protective function - free iron is cytotoxic (Beard & Connor, 2003; Fedorow et al., 2005; Zecca et al., 2002). The blood-brain barrier protects the central nervous system from fluctuations in the peripheral system (Beard & Connor, 2003; Singh et al., 2014) and in the present study, SN echogenicity could not be predicted by peripheral iron status. Furthermore, SN echogenicity did not show an association with MRI neuromelanin measures of the SN, neither with volumetric measures, nor with intensity measures. Hence, the results seem to be in contrast to the hypothesis that SN hyperechogenicity is a marker for neuromelanin depletion. Unfortunately, only neuromelanin-related data were obtained and failure to detect any correlations between the two imaging methods might be also related to the lack of central iron measures. Previous histological research found a relation between neuromelanin and SN echogenicity only in multivariate analyses when cerebral iron levels were accounted for as well. Associations of neuromelanin and iron with SN echogenicity are antagonistic and in addition neuromelanin stores iron. Increased echogenicity is then related to neuromelanin depletion and iron overload (Zecca et al., 2005). Future research addressing the nature of SN echogenic signals should include both iron-sensitive MRI measures as well as neuromelanin-sensitive MRI data to approach this question in vivo. Besides, iron levels might also influence neuromelanin signal acquisition with MRI. It has been proposed that iron can disguise neuromelanin MRI signals of the SN, especially if neuromelanin levels are low and that therefore SN iron indices should also be investigated. Disproportional high iron concentrations might saturate the MRI signal and thereby mask neuromelanin signals (Sasaki et al., 2006). Low nigral neuromelanin contents are found in PD patients but also in young children. Again, for precise approximation of neuromelanin tissue content, iron-related MRI measures should be obtained in addition. Importantly, it has been discussed that in ADHD children SN hyperechogenicity might have other morphological aspects than those proposed for adults and PD. Instead of aberrant central iron homeostasis, a developmental delay and altered functional connectivity have been

considered as possible structural candidates. Increased tissue density might then lead to the TCS signal changes that have been observed in ADHD (Drepper et al., 2017). This is further supported by the notion that ADHD children show in fact reduced - but not elevated - central iron indices (Adisetiyo et al., 2014; Cortese et al., 2012) and ADHD has repeatedly been related to a maturational delay in several central regions (e.g. Rubia, 2007; Vaidya, 2012). Consequently, altered structural maturation might be involved in childhood hyperechogenicity in general and could be another plausible explanation for the failure to detect associations with neuromelanin within this study. Alternative hypotheses concerning potential causes for SN hyperechogenicity, such as neuronal cell death, aberrant tissue composition and others, have been outlined and critically evaluated elsewhere (Double, Todd & Duma, 2010). Clearly, more research is warranted in order to elucidate this topic and comparative studies of different age groups and might be particularly useful.

A shortcoming of the study design clearly was the age-range ($8 - 12$). There was no significant association between SN echogenic signals and age in this sample. Although in fact it is possible that age does not influence SN echogenicity, to profoundly assess age-related changes in nigral signals the age range was too narrow, especially with a small sample size and most of the children effectively being aged between $9 - 11$. Previously, increases (Hagenah et al., 2010, Berg et al., 1999a) or decreases (Iova et al. 2004) of SN echogenicity with age have been found only in studies with broader age ranges. In this current study, sonographic neuroimaging of the SN was positively correlated with age, although it did not reach statistical significance. This supports the hypothesis, that echogenic characteristics might develop very early in life and that changes afterwards are subtle (Berg et al., 1999a, Berg et al., 2001b). Also in the light of altered brain iron mechanisms as potential biophysical correlates of nigral echogenicity, developmental changes in SN echogenicity of children are expected. Nigral iron concentrations increase with normal ageing from $20\ ng/mg$ in the first year to $100 - 200\ ng/mg$ in late adolescence & early adulthood (Zecca et al., 2001). Histological studies (Zecca et al., 2001; Zucca et al., 2006) as well as neuroimaging studies (Xing, 2018) have shown that nigral neuromelanin content increases with age as well. Within the first two decades of life increments

from below-detection-limits to 1000 ng/mg have been reported (Zecca et al., 2001). SN hyperechogenicity is considered to be a trait marker, that develops early (Berg et al., 1999a). This is further corroborated by the finding of this study: even in young children hyperechogenic SN sizes, that approximate adult sizes, are observed. However, to adequately map the developmental changes in SN echogenic signals a broad age range is necessary to capture the emergence of individual differences in SN echogenicity. The cross-sectional design further confines the interpretability. In general longitudinal designs are desirable to pursue questions regarding developmental changes and to detect possible developmental differences. Most of the specific limitations of this study have already been discussed and what remains are some general issues. Sample size was small, accordingly results have to be replicated in studies with more power. Inherent in the nature of correlational designs, causal inferences cannot be made. Consequently, all results have to be seen as associations and not as cause or consequence. Another obvious pitfall is that TCS image acquisition and measurement of structures critically depend on the investigators' expertise and are to some degree also a subjective measure. Additionally, image resolution can be a problem, sometimes pictures are blurry and it can be difficult to distinguish between signal and noise. Nevertheless, interrater reliability in this sample was good and suggests sufficient consistency and objectivity of the measurements.

Conclusion TCS is a convenient tool to quickly assess subcortical structures and it might be useful in longitudinal designs that investigate midbrain developmental changes in children. The origins of the echogenic signals in children hitherto have not yet been clarified, combined MRI imaging methods could be valuable for further in-vivo investigation. Dopaminergic deficits are of great clinical and scientific interest and it is an intriguing question if SN hyperechogenicity in healthy children maps nigrostriatal dysfunction. Interestingly, there is preliminary evidence that also in healthy children behavioral differences in hyperactive tendencies are associated with differences in substantia nigra echogenicity and TCS seems a promising tool to help identify children at risk of subclinical ADHD. Future studies are required to consolidate the findings.

5 Appendix

		TCS SN (cm^2)	Contrast_SN	SN Volume (cm^3)	Age (years)
Pearson Correlation	TCS SN (cm^2)	1.000	-.213	.213	.296
	Contrast_SN	-.213	1.000	.217	.317
	SN Volume (cm^3)	.213	.217	1.000	.279
	Age (years)	.296	.317	.279	1.000
Sig. (1-tailed)	TCS SN (cm^2)		.148	.148	.071
	Contrast_SN	.148		.143	.057
	SN Volume (cm^3)	.148	.143		.084
	Age (years)	.071	.057	.084	

Table 7: Correlation matrix for neuroimaging parameters and age.

		TCS SN (cm^2)	Iron (µg/dl)	Ferritin (µg/l)	Transferrin (mg/dl)	TSAT (%)
Pearson Correlation	TCS SN (cm^2)	1.000	.043	-.297	.030	.016
	Iron (µg/dl)	.043	1.000	.213	-.497	.957
	Ferritin (µg/l)	-.297	.213	1.000	-.291	.261
	Transferrin (mg/dl)	.030	-.497	-.291	1.000	-.702
	TSAT (%)	.016	.957	.261	-.702	1.000
Sig. (1-tailed)	TCS SN (cm^2)		.425	.090	.448	.473
	Iron (µg/dl)	.425		.170	.009	.000
	Ferritin (µg/l)	.090	.170		.095	.120
	Transferrin (mg/dl)	.448	.009	.095		.000
	TSAT (%)	.473	.000	.120	.000	

Table 8: Correlation matrix for serum iron parameters.

6 Abstract

Objective: Substantia nigra hyperechogenicity is found in children with attention-deficit hyperactivity disorder (ADHD). Research with transcranial sonography (TCS) in adults suggests that echogenic alterations are linked to subclinical behavioral deficits and that brain iron homeostasis is involved in the signal genesis. The purpose of this study was to explore substantia nigra echogenicity in healthy children, to assess age-related changes and to investigate whether echogenic signals relate to subclinical alterations in behavior. Furthermore, associations of central nigral neuromelanin measures and peripheral serum iron parameters to echogenic signals of the substantia nigra were evaluated. **Methods:** In a multimodal study design, neuroimaging of the substantia nigra was conducted with TCS and neuromelanin-sensitive magnetic resonance imaging (MRI) in 28 healthy children ($8 - 12\,years$). Correlations and multiple regression analyses determined associations between the neuroimaging methods, behavioral data from Strength and Difficulties Questionnaire (SDQ) and serum iron-related parameters. **Results:** Substantia nigra echogenicity correlated inversely with hyperactivity ratings in healthy, non-ADHD children ($r = -.602, p = .001$). Echogenic sizes did not change as a function of age. Neuromelanin-sensitive MRI measures of the substantia nigra and peripheral serum iron parameters were not associated with nigral TCS signals. **Conclusion:** In healthy children behavioral differences in hyperactive tendencies are associated with differences in substantia nigra echogenicity. This could help to identify those children who are at risk of subclinical ADHD.

7 Bibliography

1. Aaslid, R., Markwalder, TM., & Nornes, H. (1982). Noninvasive transcranial Doppler ultrasound recording of flow velocity in basal cerebral arteries. *J Neurosurg.* 57, 769-74.

2. Adisetiyo, V., & Helpern, JA. (2015). Brain iron: a promising noninvasive biomarker of attention-deficit/hyperactivity disorder that warrants further investigation. *Biomark Med.* 9, 403-6.

3. Adisetiyo, V., Jensen, JH., Tabesh, A., Deardorff, RL., Fieremans, E., Di Martino, A., Gray, KM., Castellanos, FX., & Helpern, JA. (2014). Multimodal MR imaging of brain iron in attention deficit hyperactivity disorder: a noninvasive biomarker that responds to psychostimulant treatment? *Radiology.* 272, 524-32.

4. Allen, RP., & Earley, CJ. (2007). The role of iron in restless legs syndrome. *Mov Disord*. 22, Suppl 18, 440-8.

5. Allen, RP., Barker, PB., Wehrl, F., Song, HK., & Earley, CJ. (2001). MRI measurement of brain iron in patients with restless legs syndrome. *Neurology*. 56, 263-265.

6. Badgaiyan, RD., Sinha, S., Sajjad, M., & Wack, DS. (2015). Attenuated Tonic and Enhanced Phasic Release of Dopamine in Attention Deficit Hyperactivity Disorder. *PLoS One*. 10, e0137326.

7. Balázs, J., & Keresztény, A. (2014). Subthreshold attention deficit hyperactivity in children and adolescents: a systematic review. *Eur Child Adolesc Psychiatry.* 23, 393-408.

8. Bear, M. F., Connors, B. W., & Paradiso, M. A. (2007). *Neuroscience: Exploring the brain* (3rd ed.). Philadelphia, PA, US: Lippincott Williams & Wilkins Publishers.

9. Beard J., & Connor, J. (2003). Iron status and neural functioning. *Ann Rev Nutr*. 23, 41–58.

10. Becker, G., & Berg, D. (2001). Neuroimaging in basal ganglia disorders: Perspectives for transcranial ultrasound. *Movement disorders*. 16, 23–32.

11. Becker, G., Bogdahn, U., Strassburg, HM., Lindner, A., Hassel, W., Meixensberger, J., & Hofmann, E. (1994a). Identification of ventricular enlargement and estimation of intracranial pressure by transcranial color-coded real-time sonography. *J Neuroimaging*. 4, 17-22.

12. Becker, G., Krone, A., Koulis, D., Lindner, A., Hofmann, E., Roggendorf, W., & Bogdahn, U. (1994b). Reliability of transcranial colour-coded real-time sonography in assessment of brain tumours: correlation of ultrasound, computed tomography and biopsy findings. *Neuroradiology*. 36, 585-90.

13. Becker, G., Perez, J., Krone, A., Demuth, K., Lindner, A., Hofmann, E., Winkler, J., & Bogdahn, U. (1992). Transcranial color-coded real-time sonography in the evaluation of intracranial neoplasms and arteriovenous malformations. *Neurosurgery*. 31, 420-8.

14. Becker, G., Seufert, J., Bogdahn, U., Reichmann, H., & Reiners, K. (1995). Degeneration of substantia nigra in chronic Parkinson's disease visualized by transcranial color-coded real-time sonography. *Neurology*. 45, 182-4.

15. Behnke, S., Schroeder, U., Dillmann, U., Buchholz, HG., Schreckenberger, M., Fuss, G., Reith, W., Berg, D., & Krick, CM. (2009). Hyperechogenicity of the substantia nigra in healthy controls is related to MRI changes and to neuronal loss as determined by F-Dopa PET. *Neuroimage*. 47, 1237-43.

16. Berg, D., Becker, G., Zeiler, B., Tucha, O., Hofmann, E., Preier, M., Benz, P., Jost, W., Reiners, K., & Lange, KW. (1999a). Vulnerability of the nigrostriatal system as detected by transcranial ultrasound. *Neurology*. 53, 1026-31.

17. Berg, D., Godau, J., & Walter, U. (2008). Transcranial sonography in movement disorders. *The Lancet Neurology*. 7, 1044-1055.

18. Berg, D., Grote, C., Rausch, WD., Mäurer, M., Wesemann, W., Riederer, P., & Becker, G. (1999b). Iron accumulation in the substantia nigra in rats visualized by ultrasound. *Ultrasound Med Biol.* 25, 901-4.

19. Berg, D., Jabs, B., Merschdorf, U., Beckmann, H., & Becker, G. (2001a). Echogenicity of substantia nigra determined by transcranial ultrasound correlates with severity of parkinsonian symptoms induced by neuroleptic therapy. *Biol Psychiatry*. 50, 463-7.

20. Berg, D., Merz, B., Reiners, K., Naumann, M., & Becker, G. (2005). Five-year follow-up study of hyperechogenicity of the substantia nigra in Parkinson's disease. *Mov Disord*. 20, 383-5.

21. Berg, D., Roggendorf, W., Schröder, U., Klein, R., Tatschner, T., Benz, P., Tucha, O., Preier, M., Lange, KW., Reiners, K., Gerlach, M., & Becker, G. (2002). Echogenicity of the substantia nigra: association with increased iron content and marker for susceptibility to nigrostriatal injury. *Arch Neurol*. 59, 999-1005.

22. Berg, D., Siefker, C., Ruprecht-Dörfler, P., & Becker G. (2001b). Relationship of substantia nigra echogenicity and motor function in elderly subjects. *Neurology*. 56, 13-7.

23. Biederman, J., & Faraone, SV. (2005). Attention-deficit hyperactivity disorder. *Lancet*. 366, 237-48.

24. Bokor, G., & Anderson, PD. (2014). Attention-Deficit/Hyperactivity Disorder. *J Pharm Pract*. 27, 336-49.

25. Bouwmans, AE., Vlaar, AM., Mess, WH., Kessels, A., & Weber, WE. (2013). Specificity and sensitivity of transcranial sonography of the substantia nigra in the diagnosis of Parkinson's disease: prospective cohort study in 196 patients. *BMJ Open*. 3.

26. Cattell, RB. (1963). Theory of fluid and crystallized intelligence: A critical experiment. *Journal of Educational Psychology.* 54, 1-22.

27. Caslake, R., Moore, JN., Gordon, JC., Harris, CE., & Counsell, C. (2008). Changes in diagnosis with follow-up in an incident cohort of patients with parkinsonism. *J Neurol Neurosurg Psychiatry*. 79, 1202-7.

28. Coghill, D,. & Sonuga-Barke, EJS. (2012) Annual research review: categories versus dimensions in the classification and conceptualisation of child and adolescent mental disorders—implications of recent empirical study. *J Child Psychol Psychiatry* 53, 469–489.

29. Connor, JR., Boyer, PJ., Menzies, SL., Dellinger, B., Allen, RP., Ondo, WG., & Earley. CJ. (2003). Neuropathological examination suggests impaired brain iron acquisition in restless legs syndrome. *Neurology.* 61, 304-9.

30. Cortese, S., Azoulay, R., Castellanos, FX., Chalard, F., Lecendreux, M., Chechin, D., Delorme, R., Sebag, G., Sbarbati, A., Mouren, MC., Bernardina, BD., & Konofal, E. (2012). Brain iron levels in attention-deficit/hyperactivity disorder: a pilot MRI study. *World J Biol Psychiatry.* 13, 223-31.

31. Dashti, M., & Chitsaz, A. (2014). Hallervorden-Spatz disease. *Adv Biomed Res*. 3, 191.

32. Del Campo, N., Chamberlain, SR., Sahakian, BJ., & Robbins, TW. (2011). The roles of dopamine and noradrenaline in the pathophysiology and treatment of attention-deficit/hyperactivity disorder. *Biol Psychiatry.* 69, 145-57.

33. Dexter, DT., Wells, FR., Lees, AJ., Agid, F., Agid, Y., Jenner, P., & Marsden, CD. (1989). Increased nigral iron content and alterations in other metal ions occurring in brain in Parkinson's disease. J *Neurochem*. 52, 1830-6.

34. Double, KL., Todd, G., & Duma, SR. (2010). Pathophysiology of transcranial sonography signal changes in the human substantia nigra. In D. Berg & U. Walter (Eds.), *Transcranial sonography in Movement disorders,* International Review of Neurobiology. 90, 107-120.

35. Dörner, K. (2009). *Klinische Chemie und Hämatologie* (7th ed.). Stuttgart, Germany: Georg Thieme Verlag.

36. Dössel, O. (2016). *Bildgebende Verfahren in der Medizin* (2nd ed.). Heidelberg, Germany: Springer Verlag.

37. Donfrancesco, R., Parisi, P., Vanacore, N., Martines, F., Sargentini, V., & Cortese, S. (2013). Iron and ADHD: time to move beyond serum ferritin levels. *J Atten Disord*. 17, 347-57.

38. Drepper, C., GeiSSler, J., Pastura, G., Yilmaz, R., Berg, D., Romanos, M., & Gerlach, M. (2017). Transcranial sonography in psychiatry as a potential tool in diagnosis and research. *World J Biol Psychiatry*. 1-13.

39. Earley, CJ., Connor, JR., Beard, JL., Malecki, EA., Epstein, DK., & Allen, RP. (2000). Abnormalities in CSF concentrations of ferritin and transferrin in restless legs syndrome. *Neurology*. 54, 1698–1700.

40. Fedorow, H., Tribl, F., Halliday, G., Gerlach, M., Riederer, P., & Double, KL. (2005). Neuromelanin in human dopamine neurons: comparison with peripheral melanins and relevance to Parkinson's disease. *Prog Neurobiol.* 75, 109-24.

41. Field, A. (2005). *Discovering Statistics Using SPSS* (2nd ed.). London, UK: SAGE Publications.

42. Gaenslen, A., & Berg, D. (2010). Early Diagnosis of Parkinson's Disease. In D. Berg & U. Walter (Eds.), *Transcranial sonography in Movement disorders,* International Review of Neurobiology. 90, 82-92. *Transcranial sonography in Movement disorders,*

43. Gaenslen, A., Unmuth, B., Godau, J., Liepelt, I., Di Santo, A., Schweitzer, KJ., Gasser, T., Machulla, HJ., Reimold, M., Marek, K., & Berg, D. (2008). The specificity and sensitivity of transcranial ultrasound in the differential diagnosis of Parkinson's disease: a prospective blinded study. *Lancet Neurol*. 7, 417-24.

44. Gazzaniga, MS., Ivry, RB., & Mangun, GR. (2009). *Cognitive neuroscience: The biology of the mind* (3rd ed.). New York: W.W. Norton.

45. Gerlach, M., Ben-Shachar, D., Riederer, P., & Youdim, MB. 1994. Altered brain metabolism of iron as a cause of neurodegenerative diseases? *J Neurochem*. 63, 793-807.

46. Godau, J., & Sojer, M. (2010). Transcranial Sonography in Restless Legs Syndrome. In D. Berg & U. Walter (Eds.), *Transcranial sonography in Movement disorders,* International Review of Neurobiology. 90, 199-215.

47. Götz, ME., Double, K., Gerlach, M., Youdim, MB., & Riederer, P. 2004. The relevance of iron in the pathogenesis of Parkinson's disease. *Ann N Y Acad Sci*. 1012, 193-208.

48. Goodman, R. (1997). The Strengths and Difficulties Questionnaire: A Research Note. *Journal of Child Psychology and Psychiatry*. 38, 581-586.

49. Hagenah, J., König, IR., Sperner, J., Wessel, L., Seidel, G., Condefer, K., Saunders-Pullman, R., Klein, C., & Brüggemann, N. (2010). Life-long increase of substantia nigra hyperechogenicity in transcranial sonography. *Neuroimage*. 51, 28-32.

50. Hayes, A. (2012). *PROCESS*, version 3.1 [software]. Department of Psychology, Ohio State University, Columbus OH, USA. Available from http://www.processmacro.org

51. Hayes, A. & Cai, L. (2007). *Behavior Research Methods*, 39, 709-722.

52. Huber, H. (2010). Transcranial Sonography- Anatomy. *Int Rev Neurobiol*. 90, 35-45.

53. Iova, A., Garmashov, A., Androuchtchenko, N., Kehrer, M., Berg, D., Becker, G., & Garmashov, Y. (2004). Postnatal decrease in substantia nigra echogenicity. Implications for the pathogenesis of Parkinson's disease. *J Neurol.* 251, 1451-4.

54. Joutsa, J., Gardberg, M., Röyttä, M., & Kaasinen, V. (2014). Diagnostic accuracy of parkinsonism syndromes by general neurologists. *Parkinsonism Relat Disord*. 20, 840-4.

55. Juneja, M., Jain, R., Singh, V., & Mallika, V. (2010). Iron deficiency in Indian children with attention deficit hyperactivity disorder. *Indian Pediatr.* 47, 955-8.

56. Kim, JY., Kim, ST., Jeon, SH., & Lee, WY. (2007). Midbrain transcranial sonography in Korean patients with Parkinson's disease. *Mov Disord*. 22, 1922-6.

57. Klasen, H., Woerner, W., Rothenberger, A., & Goodman, R. (2003). Die deutsche Fassung des Strengths and Difficulties Questionnaire (SDQ-Deu) – Übersicht und Bewertung erster Validierungs- und Normierungsbefunde. *Praxis der Kinderpsychologie und Kinderpsychiatrie.* 52, 491-502.

58. Kóbor, A., Takács, Á., Urbán, R., & Csépe, V. (2012). The latent classes of subclinical ADHD symptoms: convergences of multiple informant reports. *Res Dev Disabil.* 33, 1677-89.

59. Koeppen, AH., & Dickson, AC. (2001). Iron in the Hallervorden-Spatz syndrome. *Pedriatic Neurol*. 25, 148–155

60. Krauel, K., Feldhaus, HC., Simon, A., Rehe, C., Glaser, M., Flechtner, HH., Heinze, HJ., & Niehaus, L. (2010). Increased echogenicity of the substantia nigra in children and adolescents with attention-deficit/hyperactivity disorder. *Biol Psychiatry*. 68, 352-8.

61. Kudo, K . (2006). *Perfusion Mismatch Analyzer*, version 5.0.5358.55864 [software]. Advanced Medical Science Center, Iwate Medical University, Iwate, Japan. Available from http://asist.umin.jp/index-e.htm

62. Lambeck, J., Niesen, WD., Reinhard, M., Weiller, C., Dose, M., & Zucker, B. (2015). Substantia nigra hyperechogenicity in hypokinetic Huntington's disease patients. *J Neurol*. 262, 711-7.

63. Liman, J., Wellmer, A., Rostasy, K., Bähr, M., & Kermer, P. (2012). Transcranial ultrasound in neurodegeneration with brain iron accumulation (NBIA). *Eur J Paediatr Neurol.* 16, 175-8.

64. Loeber, R., Burke, JD., Lahey, BB., Winters, A., & Zera, M. (2000). Oppositional defiant and conduct disorder: a review of the past 10 years, part I.*J Am Acad Child Adolesc Psychiatry.* 39, 1468-84.

65. Loke, H., Harley, V., & Lee, J. (2015). Biological factors underlying sex differences in neurological disorders. *Int J Biochem Cell Biol.* 65,139-50.

66. Lücking, CH., Amtage, F., Hummel, S., Hornyak, M., Zucker, B., & Hellwig, B. (2013). Basalganglienerkrankungen. In A. Hufschmidt, C. H. Lücking & S. Rauer (Eds.) *Neurologie compact* (6th ed., pp. 337-386). Stuttgart, Germany: Georg Thieme Verlag.

67. Mann, DM., & Yates, PO. (1974). Lipoprotein pigments--their relationship to ageing in the human nervous system. II. The melanin content of pigmented nerve cells. *Brain.* 97, 489-98.

68. Marcus, DK., & Barry, TD. (2011) Does attention-deficit/hyperactivity disorder have a dimensional latent structure? A taxometric analysis. *J Abnorm Psychol.* 120, 427–442.

69. Mizuno, S., Mihara, T., Miyaoka,T., Inagaki, T., & Horiguchi, J. (2005). CSF iron, ferritin and transferrin levels in restless legs syndrome. *J Sleep Res.* 14. 43-7.

70. Noordermeer, SDS., Luman, M., Greven, CU., Veroude, K., Faraone, SV., Hartman, CA., Hoekstram PJ., Frankem B., Buitelaar, JK., Heslenfeld, DJ., & Oosterlaan, J. (2017). Structural Brain Abnormalities of Attention-Deficit/Hyperactivity Disorder With Oppositional Defiant Disorder. *Biol Psychiatry.* 82, 642-650.

71. Ogisu, K., Kudo, K., Sasaki, M., Sakushima, K., Yabe, I., Sasaki, H., Terae, S., Nakanishi, M., & Shirato H. (2013). 3D neuromelanin-sensitive magnetic resonance imaging with semi-automated volume measurement

of the substantia nigra pars compacta for diagnosis of Parkinson's disease. *Neuroradiology.* 55, 719-24.

72. Ohtsuka, C., Sasaki, M., Konno, K., Koide, M., Kato, K., Takahashi, J., Takahashi, S., Kudo, K., Yamashita, F., & Terayama,Y. (2013). Changes in substantia nigra and locus coeruleus in patients with early-stage Parkinson's disease using neuromelanin-sensitive MR imaging. *Neurosci. Lett.* 541, 93–98.

73. Okawa, M., Miwa,. H., Kajimoto, Y., Hama, K., Morita, S., Nakanishi, I., & Kondo, T. (2007). Transcranial sonography of the substantia nigra in Japanese patients with Parkinson's disease or atypical parkinsonism: clinical potential and limitations. *Intern Med*, 46. 1527-31.

74. Oner, P., Oner, O., Azik, FM., Cop, E., & Munir, KM. (2012). Ferritin and hyperactivity ratings in attention deficit hyperactivity disorder. *Pediatr Int.* 54, 688-92.

75. Oner, O., Alkar, OY., & Oner, P. (2008). Relation of ferritin levels with symptom ratings and cognitive performance in children with attention deficit-hyperactivity disorder. *Pediatr Int.* 50, 40-4.

76. Pedroso, JL., Bor-Seng-Shu, E., Felicio, AC., Braga-Neto, P., Dutra, LA., de Aquino, CC., Ferraz, HB., do Prado, GF., Teixeira, MJ., & Barsottini, OG. (2012). Severity of restless legs syndrome is inversely correlated with echogenicity of the substantia nigra in different neurodegenerative movement disorders. a preliminary observation. *J Neurol Sci.* 319, 59-62.

77. Postert, T., Lack, B., Kuhn, W., Jergas, M., Andrich, J., Braun, B., Przuntek, H., Sprengelmeyer, R., Agelink, M., & Büttner, T. (1999). Basal ganglia alterations and brain atrophy in Huntington's disease depicted by transcranial real time sonography. *J Neurol Neurosurg Psychiatry*. 67, 457-62.

78. Qiu, A., Crocetti, D., Adler, M., Mahone, EM., Denckla, MB., Miller, MI., & Mostofsky, SH. (2009). Basal ganglia volume and shape in children with attention deficit hyperactivity disorder. *Am J Psychiatry.* 166, 74-82.

79. Rasband, WS. (1997). *ImageJ* [software]. US National Institutes of Mental Health, Bethesda, Maryland, USA. Available from https://imagej.nih.gov/ij/

80. Romanos, M., Weise, D., Schliesser, M., Schecklmann, M., Löffler, J., Warnke, A., Gerlach, M., Classen, J., & Mehler-Wex, C. (2010). Structural abnormality of the substantia nigra in children with attention-deficit hyperactivity disorder. *J Psychiatry Neurosci*. 35, 55-8.

81. Rubia, K. (2007). Neuro-anatomic evidence for the maturational delay hypothesis of ADHD. *Proc Natl Acad Sci U S A*. 104, 19663-4.

82. Ryu, JH., Lee, MS., & Baik, JS. (2011). Sonographic abnormalities in idiopathic restless legs syndrome (RLS) and RLS in Parkinson's disease. *Parkinsonism Relat Disord*. 17, 201–203.

83. Sasaki, M., Shibata, E., Tohyama, K., Takahashi, J., Otsuka, K., Tsuchiya, K., Takahashi, S., Ehara, S., Terayama, Y., & Sakai, A. (2006). Neuromelanin magnetic resonance imaging of locus ceruleus and substantia nigra in Parkinson's disease. *Neuroreport*. 17, 1215-8.

84. Schmidauer, C., Sojer, M., Seppi, K., Stockner, H., Högl, B., Biedermann, B., Brandauer, E., Peralta, CM., Wenning, GK., & Poewe, W. (2005). Transcranial ultrasound shows nigral hypoechogenicity in restless legs syndrome. *Ann Neurol*. 58, 630-4.

85. Schweitzer, KJ., Behnke, S., Liepelt, I., Wolf, B., Grosser, C., Godau, J., Gaenslen, A., Bruessel, T., Wendt, A., Abel, F., Müller, A., Gasser, T., & Berg, D. (2007). Cross-sectional study discloses a positive family history for Parkinson's disease and male gender as epidemiological risk factors for substantia nigra hyperechogenicity. *J Neural Transm*. 114, 1167-71.

86. Seymour, KE., Tang X., Crocetti, D., Mostofsky, SH., Miller, MI., & Rosch, KS. (2017). Anomalous subcortical morphology in boys, but not girls, with ADHD compared to typically developing controls and correlates with emotion dysregulation. *Psychiatry Res Neuroimaging*. 261, 20-28.

87. Shaw, P., De Rossi, P., Watson, B., Wharton, A., Greenstein, D., Raznahan, A., Sharp, W., Lerch, JP., & Chakravarty, MM. (2014). Mapping the development of the basal ganglia in children with attention-deficit/hyperactivity disorder. *J Am Acad Child Adolesc Psychiatry.* 53, 780–789.

88. Singh, N., Haldar, S., Tripathi, AK., Horback, K., Wong, J., Sharma, D., Beserra, A., Suda, S., Anbalagan, C., Dev, S., Mukhopadhyay, CK., & Singh, A. (2014). Brain iron homeostasis: from molecular mechanisms to clinical significance and therapeutic opportunities. *Antioxid Redox Signal.* 20, 1324-63.

89. Skoloudík, D., Fadrná, T., Bártová, P., Langová, K., Ressner, P., Zapletalová, O., Hlustík, P., Herzig, R., & Kannovský, P. (2007). Reproducibility of sonographic measurement of the substantia nigra. *Ultrasound Med Biol.* 33, 1347-52.

90. Skoloudík, D., & Walter, U. (2010). Method and validity of transcranial sonography in movement disorders. In D. Berg & U. Walter (Eds.), *Transcranial sonography in Movement disorders,* International Review of Neurobiology. 90, 7-34.

91. Snyder, AM., & Connor, JR. (2009). Iron, the substantia nigra and related neurological disorders. *Biochim Biophys Acta*. 1790, 606-14.

92. Speer, CP. (2013). Neonatologie. In B. Koletzko (Ed.) *Kinder- und Jugendmedizin* (14th ed., pp. 49-105). Heidelberg, Germany: Springer.

93. Spiegel, J., Hellwig, D., Möllers, MO., Behnke, S., Jost, W., Fassbender, K., Samnick, S., Dillmann, U., Becker, G., & Kirsch, CM. (2006). Transcranial sonography and [123I]FP-CIT SPECT disclose complementary aspects of Parkinson's disease. *Brain*. 129, 1188-93.

94. Vaidya, CJ. (2012). Neurodevelopmental abnormalities in ADHD. *Curr Top Behav Neurosci.* 9, 49-66.

95. Walter, U. (2012). Transcranial sonography of the cerebral parenchyma: update on clinically relevant applications. *Perspectives in Medicine*, 1, 334–343.

96. Walter, U., Behnke, S., Eyding, J., Niehaus, L., Postert, T., Seidel, G., & Berg, D. (2007). Transcranial brain parenchyma sonography in movement disorders: state of the art. *Ultrasound Med Biol*. 33, 15-25.

97. WeiSS, R. H. (2006). *Grundintelligenztest Skala 2 - Revision - (CFT 20-R)*. Göttingen: Hogrefe.

98. Woerner, W., Becker, A., Friedrich, C., Klasen, H., Goodman, R., & Rothenberger, A. (2002): Normierung und Evaluation der deutschen Elternversion des Strengths and Difficulties Questionaire (SDQ): Ergebnisse einer repräsentativen Felderhebung. *Zeitschrift für Kinder- und Jugendpsychiatrie und Psychotherapie*. 30, 105-112.

99. Woydt, M., Greiner, K., Perez, J., Becker, G., Krone, A., & Roosen, K. (1996). Transcranial duplex-sonography in intracranial hemorrhage. Evaluation of transcranial duplex-sonography in the diagnosis of spontaneous and traumatic intracranial hemorrhage. *Zentralbl Neurochir.* 57, 129-35.

100. Xing, Y. (2018). Life span pigmentation changes of the substantia nigra detected by neuromelanin-sensitive MRI. *European Congress of Radiology*, Vienna, Austria.

101. Zecca, L., Berg, D., Arzberger, T., Ruprecht, P., Rausch, WD., Musicco, M., Tampellini, D., Riederer, P., Gerlach, M., & Becker, G. (2005). In vivo detection of iron and neuromelanin by transcranial sonography: a new approach for early detection of substantia nigra damage. *Mov Disord.* 20, 1278-85.

102. Zecca, L., Gallorini, M., Schünemann, V., Trautwein, AX., Gerlach, M., Riederer, P., Vezzoni, P., & Tampellini, D. (2001). Iron, neuromelanin and ferritin content in the substantia nigra of normal subjects at different ages: consequences for iron storage and neurodegenerative processes. *J Neurochem.* 2001, 76, 1766-73.

103. Zecca, L., Stroppolo, A., Gatti, A., Tampellini, D., Toscani, M., Gallorini, M., Giaveri, G., Arosio, P., Santambrogio, P., Fariello, RG., Karatekin, E., Kleinman, MH., Turro, N., Hornykiewicz, O., & Zucca FA. (2004). The role of iron and copper molecules in the neuronal vulnerability of locus coeruleus and substantia nigra during aging. *Proc Natl Acad Sci U S A.* 101, 9843-8.

104. Zecca, L., Tampellini, D., Gatti, A., Crippa, R., Eisner, M., Sulzer, D., Ito, S., Fariello, R., & Gallorini M. (2002). The neuromelanin of human substantia nigra and its interaction with metals. *J Neural Transm.* 109, 663–672.

105. Zucca, FA., Bellei, C., Giannelli, S., Terreni, MR., Gallorini, M., Rizzio, E., Pezzoli, G., Albertini, A., & Zecca, L. (2006). Neuromelanin and iron in human locus coeruleus and substantia nigra during aging: consequences for neuronal vulnerability. *J Neural Transm (Vienna).* 113, 757-67.

Danksagungen

Herzlichen Dank an Herrn Professor Marcel Romanos für die Überlassung des Themas, die grosszügige Bereitstellung aller notwendigen Ressourcen, die warmherzige Unterstützung und konstruktive Kritik. Desweiteren Dank an Herrn Dr. Carsten Drepper, Frau Dr. Susanne Neufang, Frau Dr. Julia Geissler und Frau Dr. Su-Yin Dang für jedwede Hilfe, sei sie methodologischer, inhaltlicher, organisatorischer oder zwischenmenschlicher Natur. Vielen Dank auch an Anna Reus, die ihre rare Zeit in die Korrektur dieser Arbeit gesteckt hat.

Von ganzem Herzen danken, möchte ich zudem meinen Eltern und meinem Bruder. Dafür, dass sie mir stets liebend den Rücken frei gehalten haben und noch immer frei halten. Dafür, dass sie die Liebe zur Medizin und Wissenschaft in mir geweckt und gefördert haben und mich zu jeder Zeit ermuntert haben weiter zu machen. Dafür, dass sie immer aufrichtig und interessiert an meinem Leben teilhaben. Dafür, dass sie dies alles überhaupt möglich gemacht haben.